Ov High

ANALYTICAL SOLUTIONS FOR A CONTINUUM PARALLEL-PLATE ELECTROSTATIC PROBE

Michael D. High

ARO, Inc.

May 1967

PROPULSION WIND TUNNEL FACILITY

ARNOLD ENGINEERING DEVELOPMENT CENTER

AIR FORCE SYSTEMS COMMAND

ARNOLD AIR FORCE STATION, TENNESSEE

NOTICES

ANALYTICAL SOLUTIONS FOR A CONTINUUM PARALLEL-PLATE ELECTROSTATIC PROBE

Michael D. High

ARO, Inc.

FOREWORD

The work reported herein was sponsored by Headquarters, Arnold Engineering Development Center (AEDC), Air Force Systems Command (AFSC), under Program Element 62405184, Project 5730, Task 04.

The results of research presented were obtained by ARO, Inc. (a subsidiary of Sverdrup & Parcel and Associates, Inc.), contract operator of AEDC, AFSC, Arnold Air Force Station, Tennessee, under Contract AF 40(600)-1200. The research was conducted under ARO Project No. PW5717, and the manuscript was submitted for publication on March 23, 1967.

This technical report has been reviewed and is approved.

Marshall K. Kingery
Research Division
Directorate of Plans
and Technology

Edward R. Feicht
Colonel, USAF
Director of Plans
and Technology

ABSTRACT

The theory for the flow of a weakly ionized gas through a parallel-plate, continuum, electrostatic probe is developed. The flow is separated into three distinct regions: (a) the inviscid, neutral core where electron conduction maintains the continuity of current between the two plates; (b) the viscous, quasi-neutral boundary layer in which the charged particle flow is similar to ambipolar diffusion; and (c) the one-dimensional, collision dominated, space-charge sheath. Analytical solutions, matched at the boundary of each region, are presented for the electron temperature in equilibrium with the gas temperature and for the electron temperature constant at its free-stream value. A criterion is given which may be used to determine whether electron thermal equilibrium exists through the boundary layer. It is shown that the sheath voltage drop comprises approximately 60 percent of the total plate voltage drop. The results also show a very well defined saturation current for the double probe and that this current is controlled by ion diffusion through the boundary layer. Expressions are developed from the solutions which allow the use of experimental data to determine the free-stream electron density and temperature.

CONTENTS

APPENDIXES

I. ILLUSTRATIONS

NOMENCLATURE

a	Defined by Eq. (67)
A	Defined in Eq. (13)
C	Mass fraction
C_P	Specific heat at constant pressure
D	Diffusion coefficient
E	Electric field
e	Electronic charge

f'	Blasius function, u/u_∞
J	Defined by Eq. (54)
J_1	Defined in Eq. (13)
j	Current density
K	Mobility coefficient
$\bar{k}$	Defined in Eq. (13)
k	Boltzmann's constant
$k_{n,e}$	Thermal conductivity
L	Plate length
ℓ	Width of plates
M	Particle mass
m	Ratio of mass fraction, C/C_∞
M_∞	Free-stream Mach number
n	Number density
P_r	Prandtl number, $\mu\, C_p/k_n$
p	Pressure
Q	Effective collision cross section for momentum transfer
R	Defined in Eq. (13)
S	Schmidt number, $\mu/\rho D_{in}$
T	Temperature
u, v	Velocity components
V	Electric potential
x, y	Cartesian coordinates
α	Defined in Eq. (13)
γ	Ratio of specific heats, coefficients in Eq. (24)
δ	Momentum-energy loss parameter
δ_B	Boundary-layer thickness
Δ	Defined in Eq. (13)
ϵ_0	Permittivity of vacuum
ζ	Defined in Eq. (13)
η	Transformed boundary-layer coordinate (defined on page 20)

θ	T/T_∞
λ	Electron-neutral mean free path
μ	Dynamic viscosity
ν	Electron-neutral collision frequency, kinematic viscosity
ρ	Mass density
ϕ	Intersection of the slope of the probe voltage-current curve with J_S (see Fig. 11)
ω	T_e/T
Ω	Defined in Eq. (47)

SUBSCRIPTS

a	Standard atmospheric conditions
e	Electrons
i	Ions
n	Neutrals
o	Edge of sheath
s	Saturation
t	Total
w	Wall
∞	Free-stream conditions

Note: MKS rationalized units are used in this report.

SECTION I
INTRODUCTION

In recent years there has been a great deal of interest concerning the use of electrostatic probes in plasma diagnostics. Much of this interest has been concentrated on extending the theory and use of conventional Langmuir probes (free-molecular probes) to flowing plasmas. Some of the techniques and theories for these probes may be found in Refs. 1 and 2. These probes are practical and yield fair results when used in a low density flow. As the density increases the space-charge sheath becomes collision dominated and a continuum theory is required.

The term "continuum electrostatic probe" will be used for a probe operating in a flow regime where the sheath thickness is much larger than an electron-neutral mean free path. The analysis of such a probe must then include the collision dominated sheath equations.

Numerical solutions have been obtained for the nonflowing, weakly ionized, collision dominated space-charge sheath for a spherical geometry and for a Couette flow. Notably, the numerical solution for the spherical probe was obtained by Cohen (Ref. 3) and Radbill (Ref. 4). The plane sheath for a collision dominated, weakly ionized gas has been solved by Chung (Ref. 5) for a Couette flow. The solution by Cohen is presented as an asymptotic theory for a spherical probe in the limits of (1) probe radius to Debye length ratio large, and (2) $T_i/T_e \rightarrow 0$ for arbitrary probe voltage. After reducing the pertinent equations for the above limits, Cohen numerically integrated the resulting differential equation. It should be pointed out that in Cohen's work the sheath thickness is much larger than the electron-neutral mean free path. Radbill, through a different numerical technique, extended the solution for the spherical probe to include arbitrary probe radius to Debye length ratio and arbitrary potentials. The solutions of Cohen, Radbill, and Su and Lam (Refs. 3, 4, and 6) all agree in the regions where the parameters of interest are equal. One feature that is worthy of note in these solutions is the failure to obtain a saturation current. A possible explanation of this behavior is the penetration of the electric field into regions far away from the probe. Since the analyses have been for a nonflowing plasma the field penetrates farther with increasing probe potential in order to maintain continuity and there is no sharply defined space-charge sheath edge. The solution of Cohen served as a basis for an analysis of a flowing plasma over an arbitrary body by Lam (Ref. 7). In his analysis Lam investigated the probe characteristics for a model very similar to that Chung used in his analysis of the Couette and stagnation point flow.

1

Although Lam's solution is for an arbitrary body it has to be restricted to a three-dimensional geometry for the limiting case of zero velocity since steady-state two-dimensional solutions cannot be obtained unless charge is supplied from some source. Both Lam's and Chung's solutions show that the electric field penetrates far into the flow, and it is necessary to include a region of near ambipolar diffusion which is matched to the nonconvective sheath. Lam's analysis was for an incompressible, isothermal plasma with constant properties while Chung and his co-workers have included compressibility (Refs. 8 and 5) and possible electron thermal nonequilibrium (Refs. 9 and 10). Other pertinent analyses for the stagnation point probe may be found in Refs. 1, 11, and 12 which are all similar to Lam's and Chung's work in their method of analysis.

In this paper the analysis is of a double, parallel-plate probe with the method of solution following that of Chung and Blankenship (Ref. 8). Analytical solutions have been obtained for the complete problem and the results verify the numerical work of Ref. 8. Justification is given for obtaining both an electron-neutral thermal equilibrium and frozen electron temperature solution. In Ref. 8 these are obtained; however, an incomplete form of the electron energy equation was used, and justification for the frozen electron temperature solution is not correct. An approximate relation is given here for determining electron thermal equilibrium by considering a balance of collision losses and the thermal conduction of the electrons. Relations are given which enable the results to be used with experimental data to yield information concerning the free-stream electron number density and temperature. Of particular significance is the approximate analytical solution of the collision dominated, plane sheath equations for arbitrary values of the parameters of interest.

SECTION II
FORMULATION AND BASIC ASSUMPTIONS

Many of the electrostatic probe theories developed have been for spherical geometries. Since it has been shown by Lam (Ref. 7) that the electric field penetrates far from the probe, spherical symmetry was necessary to attain undisturbed conditions far from the probe. Similar to the spherical probes is the stagnation point probe proposed by Tabbot (Ref. 11). The inherent difficulty in all of these probes is obtaining free-stream properties ahead of the bow shock from the probe data.

Because of the problems discussed above, the author initiated a study of a double probe consisting of two parallel plates. Independent of this Chung and Blankenship (Ref. 8) published a numerical solution of the same geometry.

This type of probe offers several advantages. The parallel-plate geometry provides two very distinct electrodes for a very definite description of the voltage drops. With the plates at close proximity to each other, the electric field is nearly normal to the surface everywhere and Poisson's equation is essentially one-dimensional in nature. The plates may be diverged slightly to account for the boundary layer buildup so that the strong shock problem may be either eliminated or reduced greatly.

The formulation will be based on the following assumptions:

1. The ordinary viscous boundary layer will be analyzed with a zero pressure gradient.

2. The charged particle number densities are nearly equal in the inviscid core and outer portions of boundary layer.

3. The sheath (where charge separation occurs) thickness is much smaller than the boundary-layer thickness and much larger than the electron-neutral mean free path.

4. The flow is assumed to be frozen in ionization and recombination. (Calculations are given which show the approximate range of validity for this assumption.)

5. The ions are in thermal equilibrium with the neutrals in all cases $(T_i = T)$ and K_i/K_e is assumed constant.

Within the framework of the above assumptions the neutral gas equations become:

Overall continuity:

$$\frac{\partial \rho u}{\partial x} + \frac{\partial \rho v}{\partial y} = 0 \tag{1}$$

Overall momentum:

$$\rho u \frac{\partial u}{\partial x} + \rho v \frac{\partial u}{\partial y} = \frac{\partial}{\partial y}\left(\mu \frac{\partial u}{\partial y}\right) \tag{2}$$

Neutral gas and ion energy equation:

$$\rho u C_p \frac{\partial T}{\partial x} + \rho v C_p \frac{\partial T}{\partial y} = \frac{\partial}{\partial y}\left(k_n \frac{\partial T}{\partial y}\right) + \mu \left(\frac{\partial u}{\partial y}\right)^2 \tag{3}$$

The conservation equations for the charge particles become:

Conservation of ions:

$$\rho u \frac{\partial C_i}{\partial x} + \rho v \frac{\partial C_i}{\partial y} = \frac{\partial}{\partial y}\left[\rho D_i \frac{\partial C_i}{\partial y} - \rho K_i C_i E\right] \tag{4}$$

Conservation of electrons:

$$\rho u \frac{\partial C_e}{\partial x} + \rho v \frac{\partial C_e}{\partial y} =$$

$$\frac{\partial}{\partial y} \left[\rho D_e \frac{T}{T_e} \frac{\partial}{\partial y} \left(\frac{C_e T_e}{T} \right) + \rho K_e C_e E \right] \qquad (5)$$

Electron energy:

$$\rho u C_{p_e} C_e \frac{\partial T_e}{\partial x} + \left[\rho v C_e - \rho D_e \frac{T}{T_e} \frac{\partial}{\partial y} \left(\frac{C_e T_e}{T} \right) - \rho K_e C_e E \right]$$

$$\left[C_{p_e} \frac{\partial T_e}{\partial y} + \frac{e}{M_e} E \right] = \frac{\partial}{\partial y} \left(k_e \frac{\partial T_e}{\partial y} \right)$$

$$+ \frac{3}{2} \delta \nu_e \frac{M_e}{M} n_e k \left(T_e - T \right) \qquad (6)$$

Poisson's equation:

$$\frac{\partial E}{\partial y} = \frac{e}{\epsilon_o} \left(n_i - n_e \right) = \frac{e\rho}{\epsilon_o} \left(\frac{C_i}{M_i} - \frac{C_e}{M_e} \right) \qquad (7)$$

The analysis is broken down into three regions (Fig. 1). The first is the inviscid neutral core in which the electric field is constant and the charged particles are delivered to the boundary layer because of their mobility and convection. The second region is the outer portion of the viscous boundary layer where $n_i \approx n_e$ and the flow is characterized by diffusion similar to ambipolar diffusion. The third region is the space-charge sheath in which $n_i \neq n_e$ and the convection can be neglected in the equations of motion.

SECTION III
SOLUTION TO THE PLANE SHEATH EQUATIONS

Analysis of Eqs. (4) through (7) is very difficult when $n_i \neq n_e$, but the complexity of the equations is greatly reduced if the convection terms

are neglected. In the outer portion of the sheath where quasi-neutrality is attained, the convection does not contribute to the net current to the wall. The region where charge separation occurs is very much thinner than the viscous boundary layer, and convection becomes negligible. Therefore the convection terms will be neglected in the sheath, and the equations reduce to those of a plane, collision dominated space-charge sheath.

As pointed out in Ref. 9, thermal nonequilibrium may exist between the electrons and neutrals in the boundary layer and sheath. It is shown in Section IV under what conditions this might occur in argon and air. There are two limiting conditions which cover a wide range of actual flows: equilibrium electron temperature ($T_e = T$) and frozen electron temperature ($T_e = T_{e\infty}$). Hence, the sheath equations will be solved for these two extremes. Under these conditions the electron energy equation becomes extraneous, and the plane sheath equations are:

$$\frac{\partial}{\partial y}\left[\rho\, D_i\, \frac{\partial C_i}{\partial y} - \rho\, K_i C_i E\right] = 0 \qquad (8)$$

$$\frac{\partial}{\partial y}\left[\rho\, D_e\, \frac{T}{T_e}\, \frac{\partial}{\partial y}\left(\frac{C_e T_e}{T}\right) + \rho\, K_e C_e E\right] = 0 \qquad (9)$$

$$\frac{\partial E}{\partial y} = \frac{e\,\rho}{\varepsilon_o}\left[\frac{C_i}{M_i} - \frac{C_e}{M_e}\right] \qquad (10)$$

The first two of these equations may be integrated to give:

$$\frac{e}{M_i}\left[\rho\, D_i\, \frac{\partial C_i}{\partial y} - \rho\, K_i C_i E\right] = j_i \qquad (11)$$

$$\frac{e}{M_e}\left[\rho\, D_e\, \frac{T}{T_e}\, \frac{\partial}{\partial y}\left(\frac{C_e T_e}{T}\right) + \rho\, K_e C_e E\right] = j_e \qquad (12)$$

where both currents are taken as positive for particle drift toward the wall. Since the equations are identical to those analyzed numerically in Ref. 8, the same notation will be used and the following parameters defined:

$$\alpha_{i,e} = \frac{c_{i,e}}{c_{i,e_o}} \qquad \zeta = \frac{1}{\Delta} \int_o^y \frac{\rho}{\rho_o} \, dy \qquad J_1 = \frac{j_i \Delta \rho_o^2 S}{e \, n_{e_o} \rho \mu}$$

$$\Delta = \int_o^{y_o} \frac{\rho}{\rho_o} \, dy \qquad A = \frac{e^2 \, n_{e_o} \Delta^2}{\varepsilon_o \, k \, T_o} \qquad R = \frac{\varepsilon_o \, E}{e \, n_{e_o} \Delta}$$

$$\bar{k} = \frac{j_e}{j_i} \frac{K_i}{K_e} \tag{13}$$

Substitution of Eq. (13) into Eqs. (10) through (12) gives

$$\frac{d\alpha_i}{d\zeta} - AR\alpha_i = J_1 \tag{14}$$

$$\frac{d}{d\zeta} (\alpha_e \omega) + AR\alpha_e = J_1 \bar{k} \tag{15}$$

$$\frac{dR}{d\zeta} = \alpha_i - \alpha_e \tag{16}$$

In normalizing the above equations, it has been assumed that $n_{i_o} = n_{e_o}$. Equation (16) shows that this is not exactly true $(\alpha_{i_o} \neq \alpha_{e_o})$ since the electric field is decaying through the sheath. However, to the first approximation (quasi-neutral approximation) this is correct so that the boundary conditions at $\zeta = 1.0$ are taken as

$$\alpha_{e_o} = \alpha_{i_o} = 1.0$$

The boundary conditions at the wall ($\zeta = 0$), although not exact, are taken as

$$\alpha_{e_w} = \alpha_{i_w} = 0$$

A discussion of these boundary conditions is given in Section 3.1.

6

Equations (14) and (15) can be integrated formally to give α_i and α_e as functions of the normalized electric field R and the independent variable ζ.

$$\alpha_i = \exp\left[\int_0^\zeta AR\, d\zeta\right] \cdot \int_0^\zeta J_1 \exp\left[-\int_0^\zeta AR\, d\zeta\right] d\zeta \qquad (17)$$

$$\alpha_e = \frac{1}{\omega} \exp\left[-\int_0^\zeta \frac{AR}{\omega}\, d\zeta\right] \cdot \int_0^\zeta J_1\bar{k} \exp\left[\int_0^\zeta \frac{AR}{\omega}\, d\zeta\right] d\zeta \qquad (18)$$

The quantity J_1 contains the factor $S/\rho\mu$ and is weakly dependent upon the temperature. Since the main contribution to the integrals is near the wall and the temperature does not vary greatly across the thin sheath, the ion Schmidt number is assumed constant through the sheath and equal to its value at the wall. This means that J_1 will be taken as constant through the sheath and equal to its wall value.

If the correct relationship between R and ζ were known, the integration of Eqs. (17) and (18) could be carried out to yield the solution since ω is a known function of ζ. The exact form of R requires the solution of the equations to be known; however, a reasonable approximation to R will give an approximation to α_i and α_e. These expressions for α_i and α_e in turn could be substituted into Eq. (16) and integration would provide an improved approximation to R. This procedure is simply the method of successive approximations and is commonly used in solving nonlinear differential equations. The practical success of this method depends almost entirely upon being able to obtain a very good first approximation to the function in question. The choice of the first approximation will be considered when treating specific cases.

Two cases will be solved which are of interest: (1) equilibrium electron temperature, and (2) constant electron temperature.

7

3.1 EQUILIBRIUM ELECTRON TEMPERATURE

The condition of the electron temperature equal to the ion temperature gives $\omega = 1.0$. Equations (14) and (15) may then be added and combined with Eq. (16) to give

$$\frac{d}{d\zeta}(\alpha_i + \alpha_e) - AR\frac{dR}{d\zeta} = J_1 (1 + \bar{k}) \tag{19}$$

Integration of Eq. (19) yields:

$$(\alpha_i + \alpha_e) - 2 - \frac{A}{2}(R^2 - R_o^2) = J_1 (1 + \bar{k})(\zeta - 1) \tag{20}$$

where the subscript o denotes conditions at $\zeta = 1.0$. Equation (20) is an exact algebraic equation between all the variables of the problem.

Subtracting Eq. (14) and (15) and using Eq. (16) gives:

$$\frac{d^2R}{d\zeta^2} - AR(\alpha_i + \alpha_e) = J_1 (1 - \bar{k}) \tag{21}$$

This equation along with Eq. (20) represents a second-order, nonlinear differential equation for the electric field R. An approximation to R is obtained by neglecting $d^2R/d\zeta^2$, which from Poisson's equation implies

$$\frac{d\alpha_e}{d\zeta} \simeq \frac{d\alpha_i}{d\zeta} \tag{22}$$

In the outer portion of the sheath where the flow is quasi-neutral, $\alpha_i \simeq \alpha_e$ and Eq. (22) is a good approximation. As the wall is approached the electric field becomes stronger and the ions become mobility limited such that $d\alpha_i/d\zeta$ becomes very small. The electrons are being repelled by the electric field and their density becomes low. From Eq. (15) we have

$$\frac{d\alpha_e}{d\zeta} \approx -AR\,\alpha_e \simeq 0$$

for $\alpha_e \simeq 0$.

Therefore, the second derivative of R is small over a large portion of the sheath.

Making the approximation of Eq. (22) in Eq. (21) gives:

$$(\alpha_i + \alpha_e) \simeq -\frac{J_1}{AR}(1 - \bar{k}) \tag{23}$$

It should be noted that Eq. (23) at $\zeta = 1.0$ gives the same quasi-neutral field as that obtained by letting $\alpha_i = \alpha_e$ in the outer region of the sheath. This field is discussed by Chung (Ref. 5) as becoming asymptotically correct for large A. Substitution of Eq. (23) into Eq. (20) gives:

$$\zeta \simeq \gamma_1 - \gamma_2 \, R^{-1} - \gamma_3 \, R^2 \tag{24}$$

where

$$\gamma_1 = 1 - \frac{2}{J_1 \, (1 + \bar{k})} + \frac{AR_o^2}{2J_1 \, (1 + \bar{k})}$$

$$\gamma_2 = \frac{1}{A} \left(\frac{1 - \bar{k}}{1 + \bar{k}} \right)$$

$$\gamma_3 = \frac{A}{2J_1 \, (1 + \bar{k})}$$

Equation (24) is an approximate expression for ζ in terms of R. A comparison of Eq. (24) with a numerical solution from Ref. 5 is given in Fig. 2, where J_1 and $\bar{k}$ were taken from Ref. 5, and shows that the approximation to R is in fact quite good. The highest order derivative of R has been neglected and two constants of integration have been lost. The result is that Eq. (24) does not satisfy all the necessary boundary conditions.

There is an important feature of this solution which will be utilized in the constant electron temperature solution and can be discussed at this point. Since the electric field at the probe surface is large compared to its value at the sheath edge, the ions tend to become mobility limited near the surface. This means that physically it is the drag force between the ions and neutrals that retards the ion motion and that the concentration gradients are no longer important in determining the particle flux. Equation (14) shows that for this condition we have

$$\alpha_{i_w} \simeq - \frac{J_1}{AR_w} \tag{25}$$

for the surface boundary condition ($\zeta = 0$). The approximation in Eq. (23) gives at $\zeta = 0$

$$\alpha_{i_w} + \alpha_{e_w} \simeq - \frac{J_1}{AR_w} (1 - \bar{k}) \tag{26}$$

which, for the range of $\bar{k}$ of interest, is very nearly equal to Eq. (25). It was pointed out previously that Eq. (23) becomes asymptotically correct at $\zeta = 1.0$ for large A; then in view of the above discussion, the approximation in Eq. (23) can be expected to be quite good through the entire sheath, and making $\alpha_{i_w} = 0$ causes only a small perturbation in the electric field near the probe surface.

By substituting Eq. (24) into Eqs. (17) and (18), with $\omega = 1.0$, and integrating we have

$$\alpha_i = - J_1 t^{\dfrac{\gamma_2 A}{3}} e^t \left(\frac{2\gamma_3}{3A^2} \right)^{1/3}$$

$$\int_{t_w}^{t} \left[\frac{\gamma_2 A}{3t} + 1 \right] t^{-\dfrac{(A\gamma_2 + 1)}{3}} e^{-t} \, dt \qquad (27)$$

$$\alpha_e = - J_1 \bar{k} \, t^{-\dfrac{\gamma_2 A}{3}} e^{-t} \left(\frac{2\gamma_3}{3A^2} \right)^{1/3}$$

$$\int_{t_w}^{t} \left[\frac{\gamma_2 A}{3t} + 1 \right] t^{\dfrac{A\gamma_2 - 1}{3}} e^t \, dt \qquad (28)$$

where
$$\alpha_{e_w} = 0 = \alpha_{i_w}$$
and
$$t = - \frac{2\gamma_3 A R^3}{3}$$

Equations (27) and (28) may now be made to satisfy all the boundary conditions at $\zeta = 1.0$ and $\zeta = 0$ by evaluating the constants (J_1 and $\bar{k}$) in the equations. Instead of specifying the current or voltage across the sheath, the ratio of currents ($\bar{k}$) will be chosen as the parameter; then J_1, R_w, and R_o will be found by solving the system of equations corresponding to Eqs. (27) and (28) evaluated at $\zeta = 1.0$ and Eq. (24) evaluated at $\zeta = 0$.

Equations (27) and (28) may be integrated in terms of the general Kummer function; however, it is possible in most cases to make approximations consistent with the values of the parameters of interest which permit these integrals to be expressed in simpler forms. Such approximations and the corresponding integrals are shown in Appendix II (Eqs. (II-10), (II-11), and (II-12)).

3.2 CONSTANT ELECTRON TEMPERATURE

A constant electron temperature means that ω is not constant so it is not possible to derive an approximate expression such as Eq. (24).

Examination of Eqs. (17) and (18) shows that the ion equation has the same form as in the equilibrium case and the electron equation has been changed by the appearance of the gas temperature. It may be expected from the form of these equations that the functional form of R and of the product R/ω cannot be very much different from that of the equilibrium case as given in Eq. (24). Therefore, the functional form of ζ as given in Eq. (24) is taken as the first approximation relating ζ to R,

$$\zeta = \gamma_1 - \gamma_2 R^{-1} - \gamma_3 R^2 \tag{29}$$

The coefficients (γ's) in this equation are not the same as those in Eq. (24) for the equilibrium solution. These coefficients are found by requiring that the approximation for R agrees with the true R at the end points and requiring the slope at the wall to be that given for the ion mobility limited condition. These requirements yield the following system of equations:

$$0 = \gamma_1 - \gamma_2 R_w^{-1} - \gamma_3 R_w^2$$

$$1.0 = \gamma_1 - \gamma_2 R_o^{-1} - \gamma_3 R_o^2$$

$$\left(\frac{d\zeta}{dR}\right)_w \equiv \frac{1}{\alpha_{i_w} - \alpha_{e_w}} \simeq -\frac{AR_w}{J_1(1 + \bar{k})} = \gamma_2 R_w^{-2} - 2\gamma_3 R_w$$

Solving this system of equations for γ_1, γ_2, and γ_3 yields:

$$\gamma_1 = \frac{AR_w^2}{2J_1(1 + \bar{k})} + \frac{3}{2}\frac{\gamma_2}{R_w} \tag{30a}$$

$$\gamma_2 = \frac{AR_w^2}{2J_1(1 + \bar{k})} R_o \frac{\left[1 - \dfrac{2J_1(1 + \bar{k})}{AR_w^2} - \dfrac{R_o^2}{R_w^2}\right]}{\left[1 - \dfrac{3}{2}\dfrac{R_o}{R_w} + \dfrac{1}{2}\dfrac{R_o^3}{R_w^3}\right]} \tag{30b}$$

$$\gamma_3 = \frac{A}{2J_1(1 + \bar{k})} + \frac{\gamma_2}{2R_w^3} \tag{30c}$$

Since the sheath is thin, a linear variation in the gas temperature will be used.

$$\frac{1}{\omega} = \frac{1}{\omega_\infty}\left\{\theta_w + (\theta_o - \theta_w)\,\varsigma\right\} \tag{31}$$

Using Eqs. (29) and (31) the resulting integration of Eq. (18) cannot be carried out in a closed form. Let F be defined by

$$\frac{1}{\omega}\frac{d\varsigma}{dR} \equiv F = \frac{(\theta_o - \theta_w)}{\omega_\infty}(\gamma_1 - \gamma_2 R^{-1} - \gamma_3 R^2)(\gamma_2 R^{-2} - 2\gamma_3 R)$$

$$+ \frac{\theta_w}{\omega_\infty}(\gamma_2 R^{-2} - 2\gamma_3 R)$$

An approximate expression is now chosen for F such that Eq. (18) may be integrated. We will use a curve fit to F of the form

$$F \approx G = \beta_2 R^{-2} - 2\beta_3 R \tag{32}$$

Since the main contribution to the integral in Eq. (18) occurs near $\varsigma = 0$, G will be made to agree with F at $\varsigma = 0$. Also, since F appears inside the integral of the exponent, G will be made to agree with F on

the average over the interval of integration. These conditions corre-
spond to

$$F]_{\zeta=0} = G]_{\zeta=0}$$

and

$$\int_{R_W}^{R_O} F dR = \int_{R_W}^{R_O} G dR$$

The resulting values of the constants are:

$$\beta_2 = \frac{\theta_w A R_w^2}{2 J_1 (1 + \bar{k})} \frac{R_O}{\omega_\infty} \frac{\left[1 - \frac{(\theta_O + \theta_w)}{2\theta_w} \frac{2 J_1 (1 + \bar{k})}{A R_w^2} - \frac{R_O^2}{R_w^2} \right]}{\left[1 - \frac{3}{2} \frac{R_O}{R_w} + \frac{1}{2} \frac{R_O^2}{R_w^2} \right]}$$

$$\beta_3 = \frac{A \theta_w}{2 J_1 (1 + \bar{k}) \omega_\infty} + \frac{\beta_2}{2 R_w^3}$$

Substituting Eq. (29) into Eq. (17) and Eq. (32) into Eq. (18) and inte-
grating gives:

$$\alpha_i = - J_1 \, t^{\frac{A\gamma_2}{3}} \, e^t \left(\frac{2\gamma_3}{3A^2} \right)^{1/3}$$

$$\int_{t_w}^{t} \left[\frac{\gamma_2 A}{3t} + 1 \right] t^{-\frac{A\gamma_2 + 1}{3}} e^{-t} \, dt \qquad (33)$$

$$\omega \, \alpha_e = - \, J_1 \bar{k} t^{-\frac{A\beta_2}{3\gamma_3}} \, e^{-\frac{\beta_3 t}{\gamma_3}} \left(\frac{2\gamma_3}{3A^2} \right)^{1/3}$$

$$\int_{t_w}^{t} \left[\frac{\gamma_2 A}{3t} + 1 \right] t^{\frac{A\beta_2 - 1}{3}} \, e^{\frac{\beta_3}{\gamma_3} t} \, dt \qquad (34)$$

where $\qquad t = - \dfrac{2\gamma_3 A}{3} \, R^3$

Another relation besides Eqs. (33) and (34) is needed in order to determine the three unknowns, J_1, R_0, and R_w. This relation may be derived in a manner similar to that used in obtaining Eq. (20). Adding Eq. (15) to Eq. (14) gives:

$$\frac{d}{d\zeta} \left(\alpha_i + \alpha_e \, \omega \right) - AR(\alpha_i - \alpha_e) = J_1 (1 + \bar{k}) \qquad (35)$$

Substituting in Poisson's equation and integrating gives:

$$\left(\alpha_i + \alpha_e \, \omega \right) - (1 + \omega_0) - \frac{A}{2} \left(R^2 - R_0^2 \right) = J_1 (1 + \bar{k})(\zeta - 1) \qquad (36)$$

The complete sheath solution is now obtained by letting $\bar{k}$ be a parameter and solving the three equations obtained by evaluating Eqs. (33) and (34) at $\zeta = 1.0$ and Eq. (36) at $\zeta = 0$ for the three unknowns, J_1, R_0, and R_w. Having obtained these unknowns, Eqs. (29), (33), and (34) can be used to compute distribution of the quantities across the sheath. Approximations to Eqs. (33) and (34) are given in Appendix II [Eqs. (II-16), (II-17), and (II-18)] which makes the sheath solution more amenable to numerical calculations.

3.3 SHEATH VOLTAGE

The sheath voltage can be found by integrating the electric field

$$\int_{V_w}^{V_0} dV = - \int_{0}^{y_0} E \, dy$$

which becomes for the sheath quantities

$$\frac{e}{kT_\infty} (V_O - V_w) = -A \int_0^{1.0} \theta\ R\ d\zeta \tag{37}$$

Using the linear variation for θ from Eq. (31), the voltage becomes

$$\frac{e}{kT_\infty} (V_O - V_w) = -A\ (\theta_O - \theta_w) \int_0^{1.0} \zeta\ R\ d\zeta$$

$$- A\ \theta_w \int_0^{1.0} R\ d\zeta \tag{38}$$

which may be integrated using Eq. (24) for R. Finally, we have the following expression for the sheath voltage:

$$\frac{e}{kT_\infty} (V_O - V_w) = -A\ (\theta_O - \theta_w) \left[\gamma_1 \gamma_2\ \ell n \frac{R_O}{R_w} \right.$$

$$+ \gamma_2{}^2 \left(\frac{1}{R_O} - \frac{1}{R_w} \right)$$

$$- \frac{2\gamma_1 \gamma_3}{3} (R_O{}^3 - R_w{}^3) + \frac{\gamma_2 \gamma_3}{2} (R_O{}^2 - R_w{}^2) \tag{39}$$

$$\left. + \frac{2\gamma_3{}^2}{5} (R_O{}^5 - R_w{}^5) \right] - A\ \theta_w \left[\gamma_2\ \ell n \frac{R_O}{R_w} \right.$$

$$\left. - \frac{2\gamma_3}{3} (R_O{}^3 - R_w{}^3) \right]$$

15

where the γ's are given in Eq. (24) for the electron equilibrium case and in Eq. (30) for the constant electron temperature case.

SECTION IV
BOUNDARY-LAYER SOLUTION

The region in the viscous boundary layer but outside the space-charge sheath is quasi-neutral ($n_i = n_e$). Observing this it is possible to eliminate the electric field from Eqs. (4) and (5) to give,

$$\rho u \frac{\partial m}{\partial x} + \rho v \frac{\partial m}{\partial y}$$

$$= \frac{\partial}{\partial y} \left[\frac{\rho D_i}{K_i} \frac{K_i K_e}{K_i + K_e} \frac{\partial m}{\partial y} \right.$$

$$\left. + \frac{\rho D_e}{K_e} \frac{K_i K_e}{K_i + K_e} \left(\frac{T}{T_e} \right) \frac{\partial}{\partial y} \left(\frac{m T_e}{T} \right) \right] \tag{40}$$

where $m = \dfrac{C}{C_\infty}$ and $m_i = m_e$. Since

$$\frac{K_i}{K_e} \approx \left(\frac{M_e}{M_i} \right)^{1/2}$$

then $K_i \ll K_e$ and Eq. (40) becomes,

$$\rho u \frac{\partial m}{\partial x} + \rho v \frac{\partial m}{\partial y} = \frac{\partial}{\partial y} \left\{ \rho D_i \frac{\partial}{\partial y} \left[m \left(1 + \frac{T_e}{T} \right) \right] \right\} \tag{41}$$

which is the convection-diffusion equation for the charged particles. It can be seen that Eq. (41) is similar to the neutral gas energy equation, and similar solutions may be found under certain assumptions. Before looking for similar solutions it is necessary to look at the electron energy equation since Eq. (41) is coupled to it.

4.1 DETERMINATION OF ELECTRON TEMPERATURE

Equation (6) can be written as:

$$\frac{5}{2} n_e k u \frac{\partial T_e}{\partial x} + \left[n_e M_e v - \rho D_e \frac{T}{T_e} \frac{\partial}{\partial y} \left(\frac{C_e T_e}{T} \right) - \rho K_e C_e E \right]$$

$$\cdot \left[\frac{5}{2} \frac{k}{M_e} \frac{\partial T_e}{\partial y} + \frac{e}{M_e} E \right] = \frac{\partial}{\partial y} \left(k_e \frac{\partial T_e}{\partial y} \right)$$

$$+ \frac{3}{2} \delta \nu_e \frac{M_e}{M} n_e k (T_e - T) \qquad (42)$$

where Ref. 13 gives,

$$k_e = \frac{15 \ k \ \mu}{4 \ M_e} \left(\frac{C_e T_e}{T} \right) \left(\frac{M}{M_e} \right)^{1/2}$$

Since the diffusion velocities are small, these terms are neglected and Eq. (42) reduces to,

$$\frac{5}{2} n_e k u \frac{\partial T_e}{\partial x} + \frac{5}{2} n_e k v \frac{\partial T_e}{\partial y}$$

$$\approx \frac{\partial}{\partial y} \left(k_e \frac{\partial T_e}{\partial y} \right) + \frac{3}{2} \delta \nu_e \frac{M_e}{M} n_e k (T_e - T) \qquad (43)$$

The last term in this equation is similar to the source term in the conservation of species in reacting boundary layers. In order to get similar solutions for Eq. (41) it is necessary that T_e can be expressed in a similar solution. It is obvious that if the collision term dominates, then $T_e = T$ and Eq. (41) has similar solutions. Also, if the collision frequency is small so that the collision term is negligible, then the electron temperature is frozen through the boundary layer. Similar solutions are again possible for Eq. (41) since T can be found from the solution of the neutral gas energy equation. This case is difficult to solve in general since the equation is highly nonlinear. The possibility of electron thermal nonequilibrium is known and has been investigated

for a stagnation point probe by Chung and Mullen (Ref. 10). Similar solutions might be obtained for Eq. (43) if some type of variation in the gas properties were allowed.

Let us assume a constant electron thermal conductivity and write Eq. (43) as:

$$u \frac{\partial T_e}{\partial x} + v \frac{\partial T_e}{\partial y} \simeq \frac{3}{2} \frac{\mu}{\rho} \frac{T_e}{T} \left(\frac{M}{M_e} \right)^{1/2} \frac{\partial^2 T_e}{\partial y^2}$$

$$+ \frac{3}{5} \delta \nu_e \frac{M_e}{M} (T_e - T) \qquad (44)$$

In order to determine the important terms in Eq. (44) we define,

$$u' = \frac{u}{u_\infty}; \quad v' = \frac{v}{u_\infty}; \quad x' = \frac{x}{L}; \quad y' = \frac{y}{L}; \quad T_e' = \frac{T_e}{T_{e_\infty}}; \quad T' = \frac{T}{T_\infty}$$

where, in the usual order of magnitude analysis,

$$u' \sim 0 \; [1] \qquad x' \sim 0 \; [1] \qquad \frac{T_{e_\infty}}{T} \simeq \frac{T_e'}{T'} \sim 0 \; [1]$$
$$v' \sim 0 \; [\delta_B] \qquad y' \sim 0 \; [\delta_B]$$

$$\frac{\partial}{\partial x'} \sim 0 \; [1] \qquad \frac{\partial}{\partial y'} \sim 0 \; \left[\frac{1}{\delta_B} \right]$$

and δ_B is the viscous boundary-layer thickness. The order of magnitude of the terms in Eq. (44) are then,

$$u' \frac{\partial T_e'}{\partial x'} + v' \frac{\partial T_e'}{\partial y'} \simeq \frac{3}{2} \frac{1}{R_e} \left(\frac{M}{M_e} \right)^{1/2} \frac{\partial^2 T_e'}{\partial y'^2}$$

$$+ \frac{3}{5} \delta \nu_e \frac{L}{u_\infty} \frac{M_e}{M} \left(T_e' - T \right) \qquad (45)$$

$$(1) \quad (1) + (\delta_B) \quad \frac{1}{(\delta_B)} \simeq \frac{1}{R_e} \left(\frac{M}{M_e} \right)^{1/2} \frac{1}{(\delta_B^2)}$$

$$+ \text{ collision term.}$$

18

The thickness of the viscous boundary layer is

$$\delta_B \sim 0\left(\frac{1}{\sqrt{R_{e_x}}}\right)$$

so the electron thermal conduction term is of order

$$0\left(\frac{M}{M_e}\right)^{1/2}$$

compared to unity for the convection terms. The magnitude of the collision term depends on the energy exchange between the electrons and neutrals. Equation (45) is essentially a balance between the thermal conduction and the collision loss terms and can be written as:

$$k_e \frac{\partial^2 T_e}{\partial y^2} = -\frac{3}{2} \delta\nu_e \frac{M_e}{M} n_e k (T_e - T) \tag{46}$$

When the right side dominates, $T_e = T$; when the right side is negligible, T_e = constant through the boundary layer. To develop an approximate criterion for electron thermal equilibrium we let

$$\frac{\partial^2 T_e}{\partial y^2} \simeq -\frac{T_{e_\infty} - T_{e_w}}{\delta_B{}^2} \simeq -\frac{\left(T_{e_\infty} - T_{e_w}\right)}{25 \, x^2} R_{e_x}$$

Equation 46 then reduces to

$$\frac{T_{e_w}}{T_\infty} = \frac{1}{2}\left\{(1 - \Omega) + \left[(1 - \Omega)^2 + 4\Omega\theta_w\right]^{1/2}\right\} \tag{47}$$

where

$$\theta_w = \frac{T_w}{T_\infty}$$

$$\Omega = \frac{10 \, \delta\nu_e x\theta_w}{u_\infty}\left(\frac{M_e}{M}\right)^{3/2} = 7.15 \times 10^{21} \frac{x\delta Q_{en}}{M_\infty} \frac{\rho_\infty}{\rho_a}\theta_w$$

Equation (47) is shown in Fig. 3 for two representative wall temperatures. The magnitude of Ω depends on gas flow conditions and the type of gas being used. For argon $\delta = 10$ and $Q_{en} \approx 7 \times 10^{-21}$ m^2, and for nitrogen or air δ probably lies between 10 and 100 and $Q_{en} \approx 10^{-19}$ m^2. Using the typical flow conditions of $T_\infty = 4200°K$, $p_\infty = 0.1$ atm; $M_\infty = 1$, and $\theta_w = 0.1 - 0.3$ the corresponding values of Ω for argon and air are shown. It is shown that for argon the electron temperature is nearly constant and for air ($\delta = 100$) the electron temperature is nearly in thermal equilibrium with the gas. Hence, the two extremes of equilibrium T_e and constant T_e are very representative of many flows of interest. It should be pointed out again that these expressions were developed under the assumption that the ionization and recombination are frozen.

4.2 SOLUTION FOR THE CHARGED PARTICLE CONVECTION-DIFFUSION EQUATION

Equation (41) can be solved approximately for the two cases of the electron temperature if the quantity m is assumed to vary slowly along the edge of the sheath. The equation can be transformed by

$$\eta = \left(\frac{u_\infty}{2\nu_\infty x} \right)^{1/2} \int_o^y \frac{\rho}{\rho_\infty} \, dy$$

$$\psi = (2u_\infty \nu_\infty x)^{1/2} \, f(\eta)$$

$$\frac{\rho v}{\rho_\infty} = -\frac{\partial \psi}{\partial x}; \quad \frac{\rho u}{\rho_\infty} = \frac{\partial \psi}{\partial y}; \quad \frac{df}{d\eta} = \frac{u}{u_\infty}$$

and letting $\dfrac{\rho \mu}{\rho_\infty \mu_\infty} = 1.0$. Applying this transformation yields

$$\frac{d}{d\eta} \left(\frac{1}{S} \frac{d(mg)}{d\eta} \right) + f \frac{dm}{d\eta} = 0 \qquad (48)$$

where $g = (1 + \omega)$. The boundary conditions on Eq. (48) are

$$m \, (\infty) \quad = 1.0$$

$$m \, (\eta_o) \, = m_o$$

where η_o is the sheath thickness.

Equation (48) can be written in the following form:

$$\frac{d}{d\eta}\left[\frac{1}{S}\ \frac{d(mg)}{d\eta}\right] + \frac{f}{g}\ \frac{d(mg)}{d\eta} = mf\ \frac{d\ell n\ g}{d\eta} \tag{49}$$

For equilibrium electron temperature the right side of the above equation is identically zero. For constant electron temperature g becomes a function of the gas temperature and the right side can, in general, be neglected. Neglecting the right side of the above yields:

$$\frac{d}{d\eta}\left[\frac{1}{S}\ \frac{d(mg)}{d\eta}\right] + \frac{f}{g}\ \frac{d(mg)}{d\eta} = 0 \tag{50}$$

which is to be used as an approximation to Eq. (48). Integration of Eq. (50) gives

$$mg = m_o g_o + (g_\infty - m_o g_o)\ \frac{\displaystyle\int_{\eta_o}^{\eta} Se^{-\int \frac{Sf}{g}\,d\eta}\,d\eta}{\displaystyle\int_{\eta_o}^{\infty} Se^{-\int \frac{Sf}{g}\,d\eta}\,d\eta} \tag{51}$$

The exponentials in the integrand of the above equation have their largest contribution near the wall and decay as η increases. The same type of behavior is seen in Appendix III in the approximate solution of the Blasius equation. It is shown there that reasonable approximations can be obtained by using the correct behavior of the exponentials near the wall provided that S and g do not vary greatly. Therefore the following approximations are used in Eq. (51):

$$S = S_w;\quad g = g_w$$

and

$$f = \frac{f_w''\ \eta^2}{2}$$

This gives,

$$mg = m_o g_o + (g_\infty - m_o g_o) \frac{\left[\gamma \left(\frac{1}{3}; \frac{f''_w S_w}{6g_w} \eta^3 \right) - \gamma \left(\frac{1}{3}; \frac{f''_w S_w}{6g_w} \eta_o^3 \right) \right]}{\Gamma \left(\frac{1}{3} \right) - \gamma \left(\frac{1}{3}; \frac{f''_w S_w}{6g_w} \eta_o^3 \right)}$$

(52)

The solution for the equilibrium electron temperature can be obtained by letting g = 2 everywhere in Eq. (52).

The order of the approximation made to Eq. (48) by Eq. (50) can be evaluated by formally integrating Eq. (49) and comparing the terms. It can be shown that if the following integral is much less than unity the approximation is good:

$$I = - \frac{1}{g_\infty} \int_o^\infty \frac{mf}{g} \frac{dg}{d\eta} e^{\int_o^\eta \frac{Sf}{g} d\eta} \left[\int_\eta^\infty Se^{-\int_o^\eta \frac{Sf}{g} d\eta} d\eta \right] d\eta$$

To evaluate I we let

$$\theta = \theta_w + (1 - \theta_w) f'$$

and from Eq. (52)

$$m \approx \frac{2f'}{g}$$

The integral then becomes

$$I \simeq - \frac{1}{g_\infty} \int_o^\infty mf \frac{dg}{d\eta} \frac{1 - f'}{f''} d\eta \simeq \frac{1}{6g_\infty}$$

The term neglected is on the order of 10 percent or less since $g_\infty \geq 2$, hence Eq. (50) is a good approximation to Eq. (48).

Equation (52) will be used in the matching of the boundary layer to the sheath at the outer edge of the sheath.

4.3 BOUNDARY-LAYER VOLTAGE DROP

The electric field has to be obtained from the species equations, since to the first order $n_i = n_e$ and Poisson's equation gives no information about the electric field. If we observe from Eqs. (4) and (5) that the convective portions of these are equal we obtain an equation which may be integrated from the edge of the sheath outward. This can be reduced to the following expression for the electric field:

$$
E = \frac{1}{m} \left[\frac{D_i}{K_i} \left(\left(\frac{K_i}{K_e} \right)_\infty \frac{\partial m}{\partial y} - \frac{\partial}{\partial y} \left(\frac{m \, T_e}{T} \right) \right) \right.
$$

$$
\left. + \frac{\rho_\infty}{\rho} \frac{kT_\infty}{e} \left(\frac{u_\infty}{2\nu_\infty x} \right)^{1/2} \left(\frac{K_i}{K_e} \right)_\infty J \right] \tag{53}
$$

where the integration constant has been taken to be $J = J(x)$. The J is evaluated by considering conditions at the edge of the sheath where the effects of charge and separation and convection are small; with Eqs. (11) and (12) J is found to be

$$
J = \frac{S_\infty}{en_{e_\infty}} \left(\frac{2x}{\nu_\infty u_\infty} \right)^{1/2} (j_e - j_i) \tag{54}
$$

The voltage drop from the edge of the sheath to the edge of the boundary layer, $\eta = \eta_\delta$, is given by the integration of Eq. (53),

$$
\frac{e}{kT_\infty} (V_\delta - V_0) = - \left(\frac{K_i}{K_e} \right)_\infty \left[\int_{\eta_0}^{\eta_\delta} \theta \frac{d \ln m}{d\eta} d\eta + J \int_{\eta_0}^{\eta_\delta} \frac{\theta^2}{m} d\eta \right]
$$

$$
+ \int_{\eta_0}^{\eta_\delta} \frac{\theta}{m} \left(\frac{d(\omega m)}{d\eta} \right) d\eta \tag{55}
$$

For the equilibrium case $\omega = 1$ and Eq. (55) becomes

$$\frac{e}{kT_\infty} (V_\delta - V_o) = \int_{\eta_o}^{\eta_\delta} \frac{\theta}{m} \frac{dm}{d\eta} d\eta + 0 \left[\left(\frac{M_e}{M} \right)^{1/2} \right] \quad (56)$$

To evaluate the integral we shall use θ as given by the compressible flow solution with $P_r = 1$, which is (Ref. 14),

$$\theta = \theta_w + (1 - \theta_w)f' + \frac{\gamma - 1}{2} M_\infty^2 f' (1 - f')$$

where

$$f' = \frac{u}{u_\infty}$$

Then Eq. (56) becomes,

$$\frac{e}{kT_\infty} (V_\delta - V_o) = - \theta_w \ln m_o$$

$$+ \left[(1 - \theta_w) + \frac{\gamma - 1}{2} M_\infty^2 \right] \int_{\eta_o}^{\eta_\delta} \frac{f'}{m} \frac{dm}{d\eta} d\eta$$

$$- \frac{\gamma - 1}{2} M_\infty^2 \int_{\eta_o}^{\eta_\delta} \frac{f'^2}{m} \frac{dm}{d\eta} d\eta + 0 \left(\left[\frac{M_e}{M_i} \right]^{1/2} \right) \quad (57)$$

The largest contribution to the remaining integrals occurs near $\eta = \eta_o$ since $\frac{f'}{m} \rightarrow 1$ and $\frac{dm}{d\eta}$ decays exponentially as $\eta \rightarrow \eta_\delta$. Therefore any approximations made in the evaluation of the integrals should be very good near η_o. Expansion of Eq. (52) for η near η_o gives

$$m = m_o + (1 - m_o) f_w'' \left(\frac{S_w}{2} \right)^{1/3} (\eta - \eta_o)$$

where we have used

$$\frac{3}{\Gamma\left(\frac{1}{3}\right)} \left(\frac{f_w''}{6}\right)^{1/3} = f_w''$$

which is consistent with the approximate evaluation of Eq. (52). Also,

$$f' = f_w'' \eta + 0(\eta^2)$$

If $m_o \ll 1$ and $\eta_o \ll 1$ then

$$\frac{f'}{m} \simeq \left(\frac{2}{S_w}\right)^{1/3}$$

over most of the range of integration. The first integral in Eq. (57) becomes

$$\left(1 - \theta_w + \frac{\gamma - 1}{2} M_\infty^2\right) \int_{\eta_o}^{\eta_\delta} \frac{f'}{m} \frac{dm}{d\eta} d\eta$$

$$\simeq \left(1 - \theta_w + (\gamma - 1) \frac{M_\infty^2}{2}\right) \left(\frac{2}{S_w}\right)^{1/3}$$

and the second integral becomes

$$- \frac{\gamma - 1}{2} M_\infty^2 \int_{\eta_o}^{\eta_\delta} \frac{f'^2}{m} \frac{dm}{d\eta} \simeq - \frac{\gamma - 1}{4} M_\infty^2 \left(\frac{2}{S_w}\right)^{2/3}$$

Numerical integration of a few cases has shown that these approximations are very good. Finally, the equilibrium boundary-layer voltage drop becomes

$$\frac{e}{kT_\infty} (V_\delta - V_o) \simeq - \theta_w \ln m_o + \left(1 - \theta_w + \frac{\gamma - 1}{2} M_\infty^2\right) \left(\frac{2}{S_w}\right)^{1/3}$$

$$- \frac{\gamma - 1}{4} M_\infty^2 \left(\frac{2}{S_w}\right)^{2/3} \tag{58}$$

25

The nonequilibrium boundary layer with $\omega = \dfrac{\omega_\infty}{\theta}$ in Eq. (55) can be integrated directly to give

$$\frac{e}{kT_\infty} (V_\delta - V_o) \simeq - \omega_\infty \ln \frac{m_o}{\theta_o} + 0\left(\sqrt{\frac{M_e}{M_i}}\right) \tag{59}$$

Equations (58) and (59) will be added to the sheath voltage drop to give the complete boundary-layer voltage drops.

4.4 INVISCID CORE VOLTAGE DROP

In the inviscid region we have from Eq. (53)

$$E_\infty = \frac{kT_\infty}{e} J \left(\frac{u_\infty}{2\nu_\infty x}\right)^{1/2} \frac{K_{i_\infty}}{K_{e_\infty}} \tag{60}$$

The voltage drop between the two boundary-layer edges is

$$\left(V_{\delta 1} - V_{\delta 2}\right) = - \int_{\delta_2}^{\delta_1} E_\infty dy \simeq - E_\infty \ell$$

where ℓ is the distance between the plates. Hence, across the inviscid core

$$\frac{e}{kT_\infty} \left(V_{\delta 1} - V_{\delta 2}\right) = - J\left(\frac{\ell}{2x}\right)^{1/2} \left(\frac{u_\infty \ell}{\nu_\infty}\right)^{1/2} \frac{K_{i_\infty}}{K_{e_\infty}} \tag{61}$$

If the integration in Eq. (61) is from the more negatively biased plate toward the more positive plate, the voltage drop in Eq. (61) will be positive.

The voltage drop across the inviscid core may or may not be negligible with respect to the total probe voltage. The voltage drop between the plates, neglecting the inviscid core, $(V_{w1} - V_{w2})$, can be written as

$$\frac{e}{kT_\infty} \left(V_{w1} - V_{w2}\right) = \frac{\varphi_s}{J_s} J \tag{62}$$

It is shown in Section VI that

$$\frac{\varphi_s}{J_s} \approx \frac{2.10\,\dfrac{T_{e_\infty}}{T_\infty}}{\left(1 + \dfrac{T_{e_\infty}}{T_\infty}\right) f_w'' \left(\dfrac{S_w\,T_w}{T_w + T_{e_\infty}}\right)^{1/3}}$$

so that

$$\frac{e}{kT_\infty}\left(V_{w1} - V_{w2}\right) \simeq \frac{2.10\,\dfrac{T_{e_\infty}}{T_\infty}}{\left(1 + \dfrac{T_{e_\infty}}{T_\infty}\right) f_w'' \left(\dfrac{S_w\,T_w}{T_w + T_{e_\infty}}\right)^{1/3}}\,J$$

Therefore

$$\left[\left(V_{\delta 1} - V_{\delta 2}\right)\right] \ll \left[\left(V_{w1} - V_{w2}\right)\right]$$

whenever

$$\left(\frac{\ell}{2x}\right)^{1/2}\left(\frac{u_\infty \ell}{\nu_\infty}\right)^{1/2} \ll 10^3\,\frac{\dfrac{T_{e_\infty}}{T_\infty}}{\left(1 + \dfrac{T_{e_\infty}}{T_\infty}\right)\left(\dfrac{S_w\,T_w}{T_w + T_{e_\infty}}\right)^{1/3}}$$

(63)

and the inviscid core voltage drop may be neglected. When this inequality is not satisfied, Eq. (61) may be used to compute the inviscid core voltage drop and it must be included in the overall probe voltage.

SECTION V
MATCHING OF THE SHEATH AND BOUNDARY LAYER

Solutions have been given for the sheath and boundary layer; it remains to match these at the edge of the sheath to complete the solution.

In matching the boundary-layer solution to the sheath solution, three conditions can be specified. These are taken to be that the electric field,

the number density of charged particles, and the electric current are all continuous at $\eta = n_0$.

The continuity of current has already been assured by the choice of the integration constant in Eq. (53). By comparing Eq. (54) to Eq. (13), this corresponds to

$$J = \frac{m_0}{\eta_0} \frac{S_\infty}{S_w} J_1 \left[\frac{j_e}{j_i} - 1 \right] \tag{64}$$

which is the form to be used here.

The continuity of the number density of charged particles has been assured by specifying that α_i and α_e are unity at the edge of the sheath. By comparing Eq. (53) with the difference between Eqs. (11) and (12), it is found that the electric field is continuous provided the quantity $\frac{dm}{d\eta}$ is continuous at $\eta = n_0$. This will now be done for the two cases considered.

For the boundary-layer solution, we have from Eq. (52)

$$\left(\frac{dm}{d\eta} \right)_0 = \frac{1}{g_0} \left(\frac{d(mg)}{d\eta} \right)_0 - \frac{m_0}{g_0} \left(\frac{dg}{d\eta} \right)_0$$

$$= \left(\frac{g_\infty}{g_0} - m_0 \right) f_w'' \left(\frac{S_w}{g_w} \right)^{1/3} - \frac{m_0}{g_0} \left(\frac{dg}{d\eta} \right)_0$$

The sheath conditions can be expressed from Eq. (35)

$$\left(\frac{dm}{d\eta} \right)_0 = J_1 \frac{m_0}{\eta_0} \frac{(1 + \bar{k})}{g_0} - \frac{m_0}{g_0} \left(\frac{d\omega}{d\eta} \right)_0$$

where α_{i_0}, $\alpha_{e_0} = 1.0$ and $1 + \omega_0 = g_0$ have been used. The last terms of the above equations are identical; the matching of the derivatives at $\eta = \eta_0$ then gives

$$J_1 \frac{m_0}{\eta_0} \frac{(1 + \bar{k})}{g_0} = \left(\frac{g_\infty}{g_0} - m_0 \right) f_w'' \left(\frac{S_w}{g_w} \right)^{1/3} \tag{65}$$

The nondimensional current from Eq. (64) then becomes

$$J = \frac{g_\infty}{1 + \bar{k}} \left(1 - \frac{m_o g_o}{g_\infty}\right) f_w'' \left(\frac{S_w}{g_w}\right)^{1/3} \frac{S_\infty}{S_w} \left[\bar{k} \left(\frac{K_i}{K_e}\right)_\infty^{-1} - 1\right] \quad (66)$$

Introducing the parameter

$$a = \frac{e^2 n_{e_\infty}}{\epsilon_o k T_\infty} \frac{2\nu_\infty x}{u_\infty}$$

into the solution we have the relation

$$\frac{A}{a} = m_o \eta_o^2 \quad (67)$$

Substituting Eq. (67) into Eq. (65) gives

$$\eta_o^3 \left[1 - \frac{A}{a} \frac{g_o}{g_\infty \eta_o^2}\right] = \frac{J_1 (1 + \bar{k})}{g_\infty} \frac{A}{a} \frac{1}{f_w''} \left(\frac{g_w}{S_w}\right)^{1/3} \frac{S_w}{S_\infty} \quad (68)$$

from which the sheath thickness can be found for a J_1 and $\bar{k}$ from the sheath solutions. Equation (68) contains a term with g_o which is a function of η_o, however this term is usually negligible. For equilibrium $g_o = 2$ and for constant electron temperature

$$g_o = 1 + \frac{\omega_\infty}{\theta_o}$$

where

$$\theta_o = \theta_w + \left\{(1 - \theta_w) + \frac{\gamma - 1}{2} M_\infty^2\right\} f_w'' \eta_o$$

For a given set of the parameters a, A, $\bar{k}$, S, ω_∞ and θ_w the current and voltage through the boundary layer are found.

SECTION VI
RESULTS

Analytical solutions are given for the flow of a weakly ionized gas between two conducting plates. The solutions are given for the particular

conditions of (1) equilibrium electron temperature, and (2) constant electron temperature through the sheath and boundary layer.

Typical sheath solutions for the charge particle density and electric field profiles are shown in Figs. 4 and 5. Figure 4 also gives a comparison with an exact numerical solution for the same set of parameters and assumptions as taken from Ref. 5. The agreement is very good. This same type of agreement was found for the entire range of parameters given in Ref. 5, indicating that the analytical solution is valid over the entire range of parameters of interest. Figure 5 also gives a comparison with an exact numerical solution of the nonequilibrium sheath as given in Ref. 8. The analytical results are for a constant electron temperature and a linear gas temperature profile while the numerical results included an approximate electron energy equation and solved for the electron temperature. The agreement between the two solutions is very good despite the assumed constant electron temperature in the analytical solution.

The sheath voltage as calculated by Eq. (39) for an equilibrium sheath is shown in Fig. 6. An isothermal and a linear gas temperature profile are shown in order to give the effect of compressibility on the sheath voltage. Direct comparison with the numerical solution from Ref. 5 is again made for the isothermal sheath, and the agreement is very good. The effect of the density variation is to decrease the voltage required to produce a given current. Since the electrons are in equilibrium with the gas, their energy is decreasing through the sheath. Therefore, it takes less voltage to decrease the electron current and keep the same net current.

Having demonstrated the validity of the sheath solutions, they are matched to the boundary-layer solution to give the complete solution. Typical profiles of the complete solution are shown in Figs. 7a and b. It can be seen that the constant electron temperature sheath is thicker than the equilibrium sheath. The electric field decays very rapidly through the sheath, with the value at the edge of the sheath being approximately one-tenth the value at the wall.

Although the electric field is weak in the boundary layer, the voltage drop is not negligible because of the much larger distance involved. This is illustrated in Fig. 8 which shows the sheath and boundary-layer voltage drops for the case of a constant electron temperature and an equilibrium electron temperature. The voltage drop across the sheath is seen to be approximately 60 percent of the total. Figure 8 also shows a very well defined saturation current for the probe. The equilibrium boundary-layer voltage is a function of the free-stream Mach number through the gas temperature dependence. Equation (58) shows that boundary-layer voltage drop increases with increasing free-stream Mach number.

The sheath thickness increases with a decrease in the free-stream electron density since the sheath thickness is characterized by (not equal to) the Debye length which increases with a decrease in electron density. This variation of the sheath thickness with n_{e_∞} (n_{e_∞} is proportional to the parameter a) is shown in Fig. 9. It is again noted that the constant electron temperature sheath is thicker than the equilibrium electron temperature sheath. A discussion in Appendix IV indicates that the solution is valid (i.e., convection need not be considered) for a sheath thickness $\eta_0 < 1.4$. Figure 10 shows the sheath thickness to be directly proportional to the sheath voltage.

The current-voltage characteristics for the double parallel-plate probe may be constructed from the total current-voltage curves such as the ones shown in Fig. 8. If the lower plate is at a negative potential with respect to the plasma, it will draw an excess ion current. The upper plate is then less negative with respect to the plasma and will draw less ion current. From the continuity of current we have that $J_\ell(x) = -J_u(x)$; hence the probe voltage is found by subtracting the voltages in Fig. 8 at J and -J. Figure 11 shows these probe voltages for several values of the parameters, T_{e_∞}/T_∞ and S_w.

It takes a much larger voltage to saturate the current when T_{e_∞}/T_∞ is larger than one. In most cases the saturation current may be found from Eq. (66) by neglecting $\dfrac{m_0 g_0}{g_\infty}$. This gives, as $\bar{k} \longrightarrow 0$,

$$J_s = -\left(1 + \frac{T_{e_\infty}}{T_\infty}\right) f_w'' \left(\frac{S_w \, T_w}{T_w + T_{e_w}}\right)^{1/3} \frac{S_\infty}{S_w} \tag{69}$$

The free-stream electron density is found from Eq. (54)

$$n_{e_\infty} = \frac{\dot{S}_\infty}{-J_s \, e} \left(\frac{2x}{\nu_\infty \, u_\infty}\right)^{1/2} j_s \tag{70}$$

Knowledge of T_{e_∞}/T_∞ is required in Eq. (69) to determine J_s for use in Eq. (70). For most cases this ratio will be unity; when the ratio is different than unity it can be evaluated from the slope of the current-voltage curve at zero current. The saturation voltage increases with T_{e_∞}/T_∞, and the slope of the characteristic curve is a function of T_{e_∞}/T_∞ as was seen previously. Using a method given by Chung and

31

Blankenship (Ref. 8) a correlation for T_{e_∞}/T_∞ can be found. A straight line is drawn with a slope equal to the characteristic curve slope at $J = 0$ from the origin until it intersects J_S. This voltage is denoted ϕ_S in Fig. 11. It is found that ϕ_S can be related to T_{e_∞}/T_∞ by

$$\frac{T_{e_\infty}}{T_\infty} = \frac{\varphi_S}{2.10} \tag{71}$$

which is very nearly equal to the value given in Ref. 8, even though the saturation currents differ considerably. It should be noted that the voltage drop in the inviscid core has been neglected in these figures, but it may not always be negligible.

In order to demonstrate the use of experimental data in Eqs. (69) and (71), by assuming a typical flow condition and probe dimensions, Fig. 12 shows the dimensional current-voltage curve one could expect to obtain experimentally. The regions of interest are marked on the curve. Also, to aid in choosing instrumentation for such a probe, the saturation current is shown as a function of free-stream electron density in Fig. 13. The parameter σ is a function only of the neutral gas flow variables and T_{e_∞}/T_∞. Conservative estimates of the current density may be made by letting $T_{e_\infty}/T_\infty = 1.0$ in σ. The condition from Fig. 12 is shown for comparison.

Both Eqs. (69) and (70) depend on the ion Schmidt number. This is a result of the saturation current being dominated by ion diffusion. Therefore, a knowledge of ion-neutral diffusion coefficient is required. The first approximation to the binary diffusion coefficient is given by Demetriades and Argyropoulos (Ref. 15) as

$$D_{in} = \frac{3}{2} \sqrt{\frac{n_n kT}{M_n}} \frac{1}{n_n^{3/2} Q_{in}}$$

where Q_{in} is the effective collision cross section for momentum transfer. This expression can be written as

$$D_{in} = 2 \times 10^{-27} \frac{T^{3/2}}{p} \frac{1}{Q_{in}} \frac{m^2}{sec} \tag{72}$$

where T is in °K; p is in atm and Q_{in} is in m^2. Not much information is available on ion-neutral collision cross sections. It is noted (Ref. 16) that the collision cross sections are approximately three times the neutral-neutral collision cross sections for most species of air. Also, the magnitude does not vary too greatly from specie to specie, hence we take

$$Q_{in} \simeq 4.36 \times 10^{-17} \, T^{-1/2} \tag{73}$$

for the effective collision cross section. The square root dependence on temperature is a result of using inverse fifth-power law interactions which are characteristic of a simple polarizable particle. Using Eqs. (72) and (73) in the definition of the ion Schmidt gives,

$$S \equiv \frac{\mu}{\rho D_{in}} = 6.44 \times 10^7 \, \frac{\mu}{T} \tag{74}$$

where μ is in Kg/m-sec and T is in °K. Figure 14 shows the variation of Eq. (74) for argon and nitrogen as a function of temperature. The viscosity of the neutral gases was calculated using viscosity data and a Lennard-Jones potential (Argon in Ref. 17 and Nitrogen in Ref. 18). If a linear viscosity law is used, consistent with the $\rho\mu$ = constant approximation, the Schmidt number is a constant. Clearly, the best available cross section or diffusion data should be used in the probe theory when interpreting experimental data.

SECTION VII
CONCLUSIONS

An electrostatic probe has been analyzed for a flow regime in which the sheath is collision dominated. The probe consists of a double parallel-plate arrangement with the actual current-carrying segments being far from the leading edge. The aerodynamic boundary layer is included in the analysis along with the continuity and energy equations of the charged particles.

Analytical solutions have been obtained for this problem. From these solutions relations have been obtained which allow the determination of the free-stream electron density and temperature from experimental probe data (see Eqs. (70) and (71)).

It is shown that the flow consists of three regions: (1) the inviscid core where the electric field is very weak and the current is by electron conduction which serves to maintain continuity between the plates,

(2) the viscous boundary layer in which the controlling mechanism is ion diffusion and is similar to ambipolar diffusion except that there is a finite current flow, and (3) the space-charge sheath across which ion diffusion and conduction play equal roles. It is found that this latter region contains very large electric field gradients and hence a large part of the voltage drop.

The saturation current is dominated by ion diffusion, and accurate knowledge of the ion-neutral diffusion coefficients is required for the particular gas being investigated. If measurements of n_{e_∞} and T_{e_∞}/T_∞ can be obtained from other sources, the continum electrostatic probe could be used in reverse and predict ion-neutral diffusion coefficients.

The range of free-stream electron density for which the theory developed is applicable is discussed in Appendix IV. Although the validity of several of the assumptions depends on the particular flow (such as the ratio of boundary-layer thickness to sheath thickness) it appears that the probe may be used in the range of $10^8/cm^3 < n_{e_\infty} < 10^{12}/cm^3$. These figures are approximate and depend upon the particular flow conditions being considered.

REFERENCES

1. Brundin, C. L.   The Application of Langmuir Probe Techniques to Flowing Ionized Gases.   Ph. D.   Dissertation, University of California (also AS-64-9).

2. Chen, F. F.   Probe Techniques.   Princeton University Press, Princeton, New Jersey, 1962.

3. Cohen, I. M.   Theory of Spherical Electrostatic Probes in a Slightly Ionized, Collision-Dominated Gas Review and Extension.   Ph. D.   Dissertation, Princeton University, 1963.

4. Radbill, J. R.   "Theory of Continuum Spherical Electrostatic Probes for Arbitrary Potential and Radius-Debye Length Ratios."   North American Aviation, Inc. Report, February 12, 1965.

5. Chung, P. M.   "Electrical Characteristics of Couette and Stagnation Boundary-Layer Flows of Weakly Ionized Gases."   Physics of Fluids, 1, Vol. 7, January 1964.

6. Su, C. H. and Lam, S. H.   "Continuum Theory of a Spherical Electrostatic Probe."   Physics of Fluids, 10, Vol. 6, October 1963.

7. Lam, S. H. "A General Theory for the Flow of Weakly Ionized Gases." Princeton University Report No. 644, April 1963 (also AIAA Preprint 63-459).

8. Chung, P. M. and Blankenship, V. D. "Theory of Electrostatic Double Probe Comprised of Two Parallel Plates." BSD-TR-65-383, April 1965 (Contract No. AF 04(695)-469.

9. Chung, P. M. "Weakly Ionized Nonequilibrium Viscous Shock-Layer and Electrostatic Probe Characteristics." AIAA Journal, 5, Vol. 3, May 1965.

10. Chung, P. M. and Mullen, J. F. "Nonequilibrium Electron Temperature Effects in Weakly Ionized Stagnation Boundary Layers." AIAA Preprint No. 63-161, June 17-20, 1963.

11. Talbot, L. "Theory of the Stagnation-Point Langmuir Probe." Physics of Fluids, 2, Vol. 3, March 1960.

12. Sonin, A. A. "Langmuir Probe Measurements in the Stagnation Point Boundary Layer of a Blunt-Nosed Body in a Supersonic Plasma Flow." UTIA TN-58, AFOSR2430, June 1963.

13. Hansen, C. F. "Approximations for the Thermodynamic and Transport Properties of High-Temperature Air." NASA TR R-50, 1959.

14. Schlichting, H. Boundary Layer Theory. McGraw-Hill Book Company, Inc., New York, 1960.

15. Demetriades, S. T. and Argyropoulos, G. S. "Ohm's Law in Multicomponent Non-Isothermal Plasmas with Temperature and Pressure Gradients." Research Report STD-65-12, September 1965.

16. Hansen, C. F. "Approximations for the Thermodynamic and Transport Properties of High Temperature Air." NACA TN 4150, March 1958.

17. Hirschfelder, J. O., Curtiss, C. F., and Bird, R. B. Molecular Theory of Gases and Liquids. John Wiley and Sons, Inc., New York, 1954.

18. Baulknight, C. W. "The Calculations of Transport Properties at Elevated Temperatures." Proceedings of the Second Biennial Gas Dynamics Symposium, Northwestern University Press, 1958.

19. Byron, S., Bortz, P. I., and Russell, G. R. "Electron-Ion Reaction Rate Theory: Determination of the Properties of Nonequilibrium Monatomic Plasmas in MHD Generators and Accelerators and in Shock Tubes." Proceedings of Fourth Symposium on Engineering Aspects of MHD, 1963.

BIBLIOGRAPHY

1. Su, C. H. "Compressible Plasma Flow over a Biased Body." AIAA Journal, 5, Vol. 3, May 1965.

2. Cohen, I. M. "Asymptotic Theory of Spherical Electrostatic Probes in a Slightly Ionized Collision-Dominated Gas." Physics of Fluids, 10, Vol. 6, October 1963.

3. Fay, J. A. "Plasma Boundary Layers." Fourth Biennial Gas Dynamics Symposium, Northwestern University, Paper No. 20-10-61, August 23-25, 1961.

4. Wasserstrom, Elishu, Su, C. H. and Probstein, R. F. "Kinetic Theory Approach to Electrostatic Probes." Physics of Fluids, 1, Vol. 8, January 1965.

5. Bienkowski, G. K. "The Transitional Electrostatic Sheath." AIAA Preprint No. 66-6, January 1966.

6. Waymouth, J. F. "Perturbation of a Plasma by a Probe." Physics of Fluids, 11, Vol. 7, November 1964.

7. Dickson, L. D. "Survey of Diagnostic Techniques Used to Determine Temperature and Density in Plasmas." The Johns Hopkins University Radiation Laboratory, AD 275762.

8. Cohen, C. B. and Reshotko, E. "Similar Solutions for the Compressible Laminar Boundary Layer with Heat Transfer and Pressure Gradient." Recent Advances in Heat and Mass Transfer, J. P. Hartnett, Editor, McGraw-Hill Book Company, Inc., N. Y., 1961.

9. Sutton, G. W. and Sherman, A. Engineering Magnetohydrodynamics. McGraw-Hill Book Company, Inc., N. Y., 1965.

10. Meksyn, D. New Methods in Laminar Boundary-Layer Theory. Pergamon Press, 1961.

11. Handbook of Mathematical Functions. NBS, AMS-55, Edited by Abramowitz, A. and Stegun, I. A., June 1964.

12. Calcote, H. F. "Relaxation Processes in Plasma." Proceedings of the Third Biennial Gas Dynamics Symposium, Northwestern University Press, 1960.

APPENDIXES

Flow →

Inviscid Core $\quad n_{i_\infty} = n_{e_\infty}$

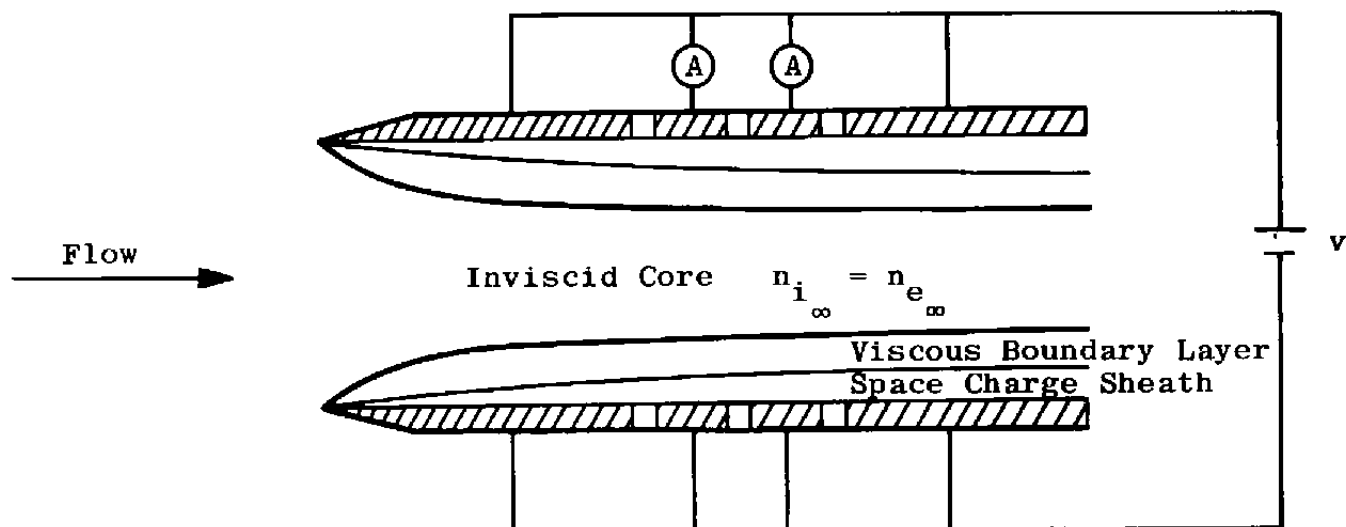Viscous Boundary Layer
Space Charge Sheath

Ⓐ Ⓐ

V

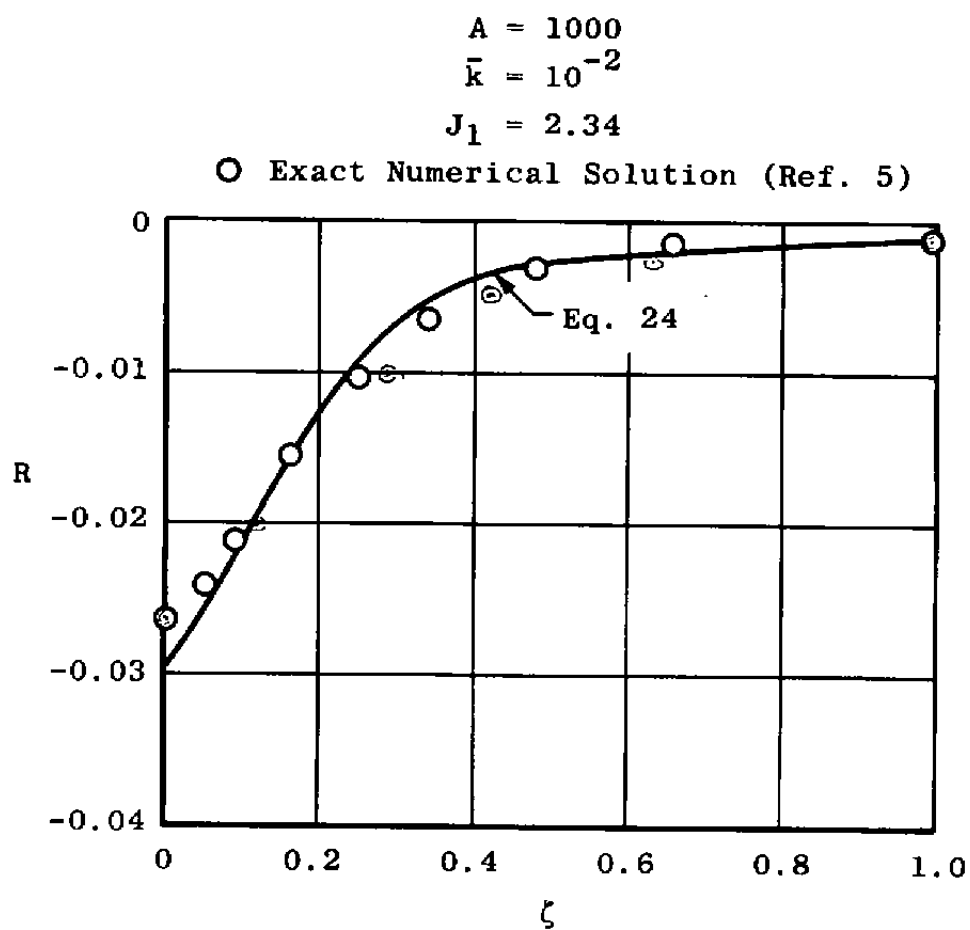Fig. 1 Schematic of Probe and Flow Regions Analyzed

Fig. 2 Comparison of Eq. (24) and Exact Numerical Solution
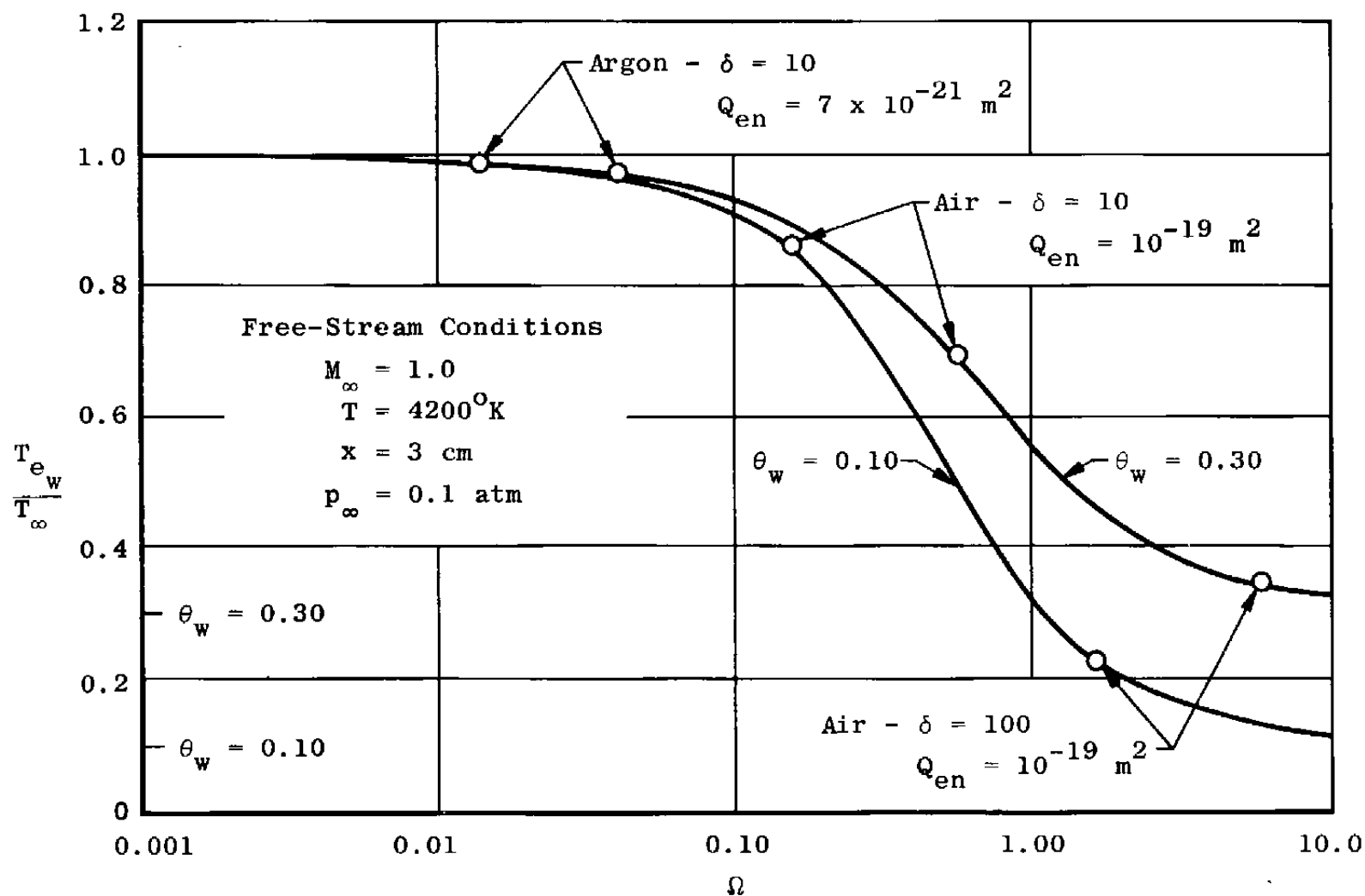Using J_1, A, and $\bar{k}$ from Ref. 5

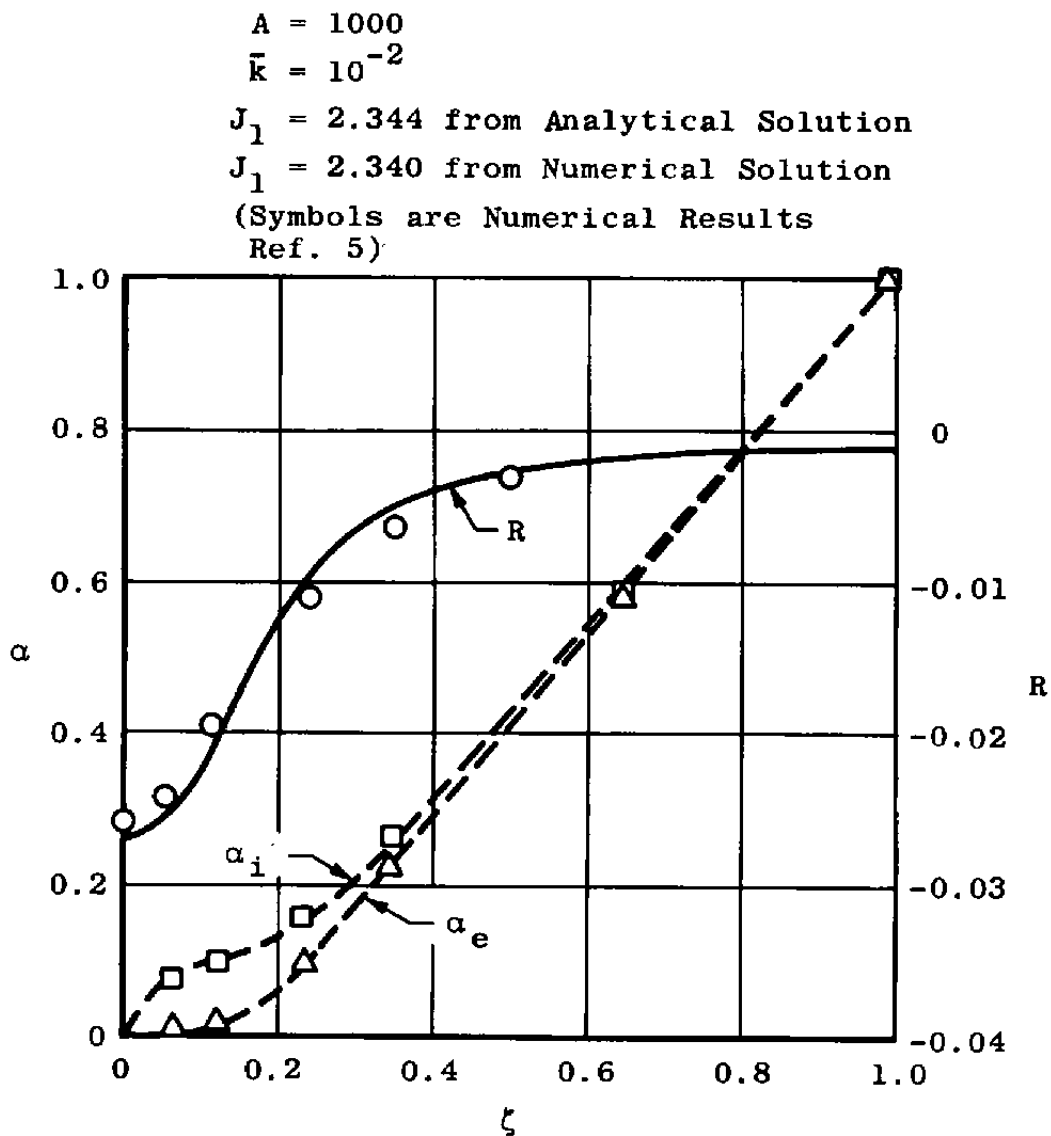Fig. 3 Degree of Electron Thermal Nonequilibrium in the Boundary Layer Assuming Equilibrium in Free Stream

$A = 1000$

$\bar{k} = 10^{-2}$

$J_1 = 2.344$ from Analytical Solution

$J_1 = 2.340$ from Numerical Solution

(Symbols are Numerical Results
Ref. 5)

Fig. 4 Equilibrium Electron Temperature Sheath Profiles

A = 3540

$\bar{k} = 7.1 \times 10^{-4}$

$\omega_\infty = 3.85$
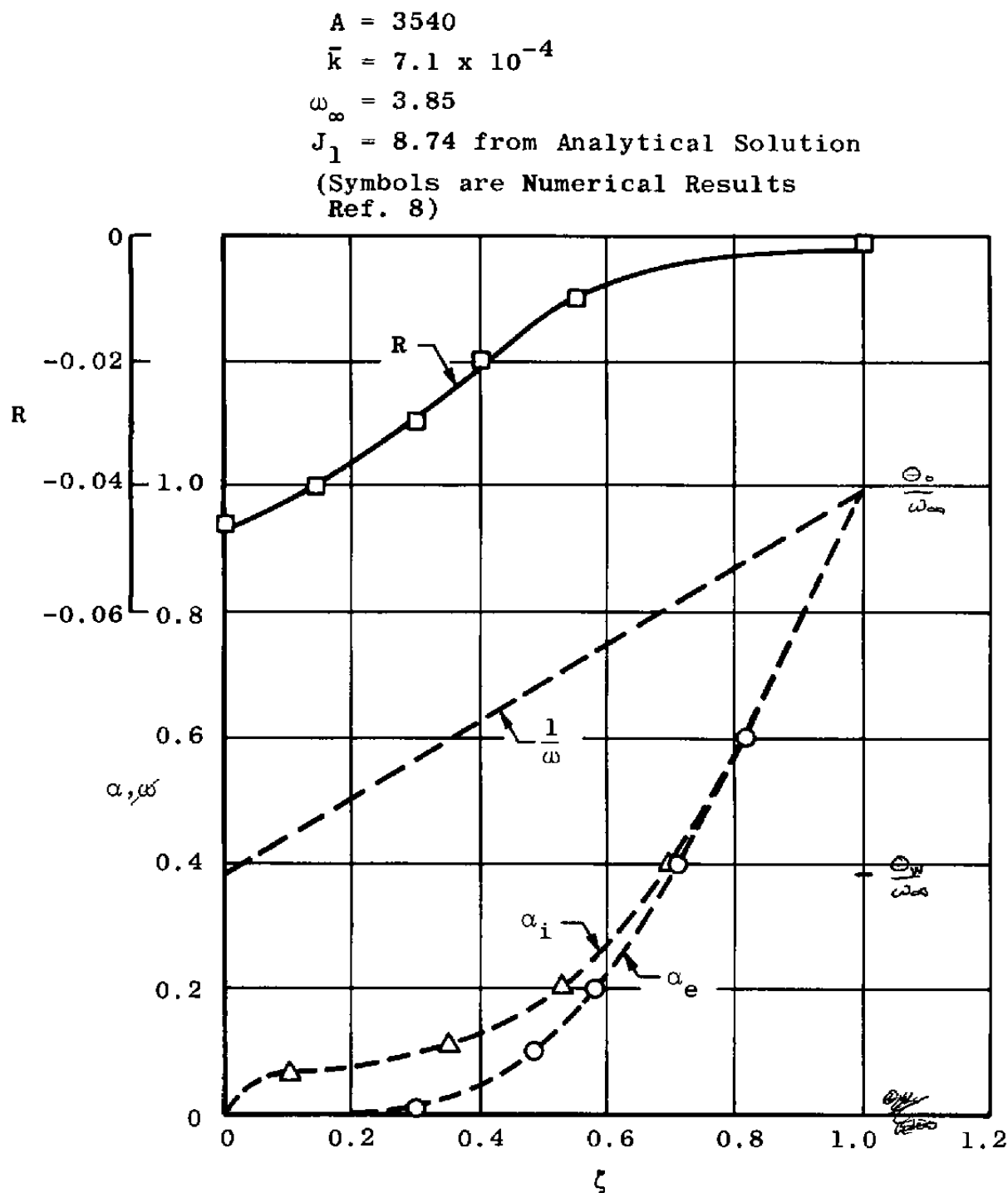
$J_1 = 8.74$ from Analytical Solution

(Symbols are Numerical Results
Ref. 8)

Fig. 5 Constant Electron Temperature Sheath Profiles
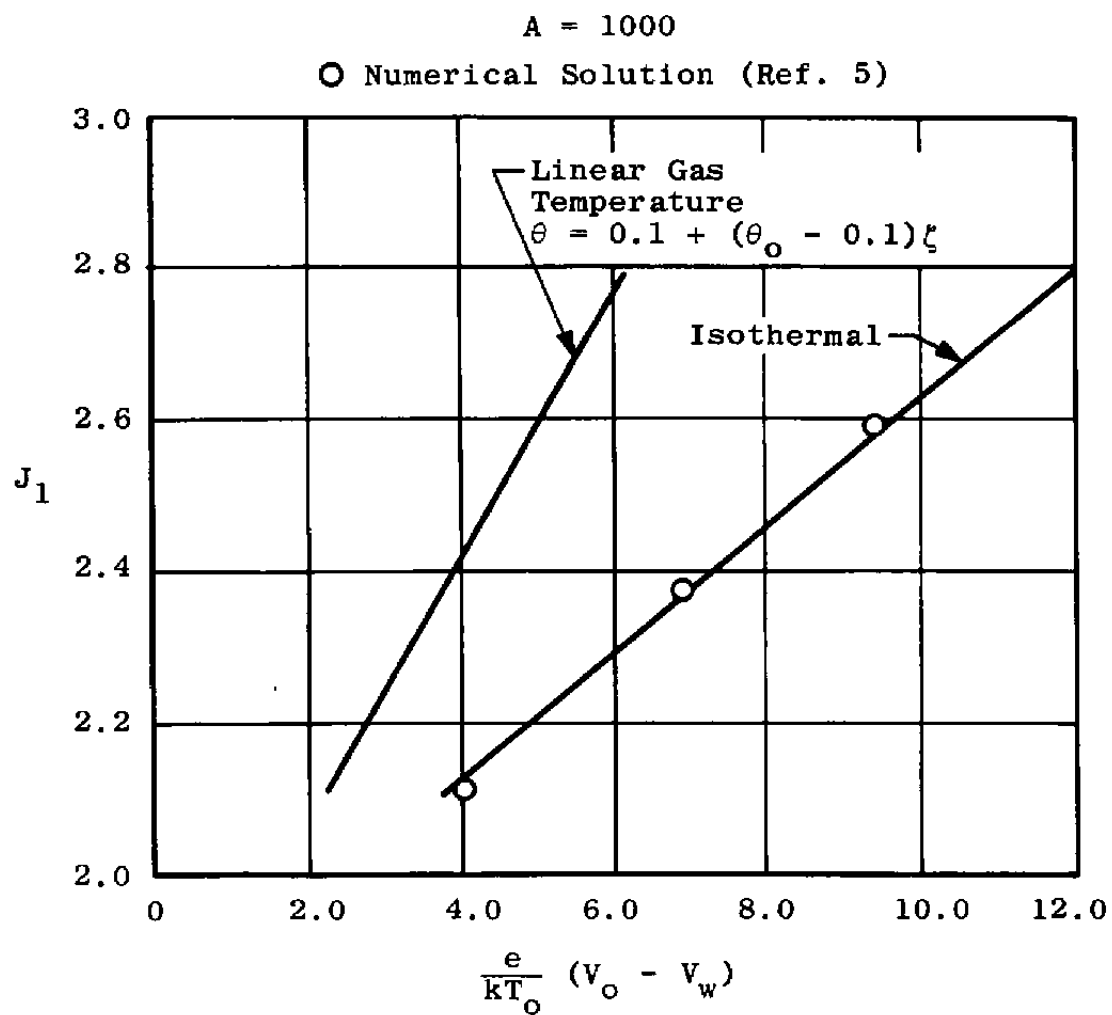
Fig. 6 Variation of Sheath Voltage with Gas Temperature for an Equilibrium Sheath

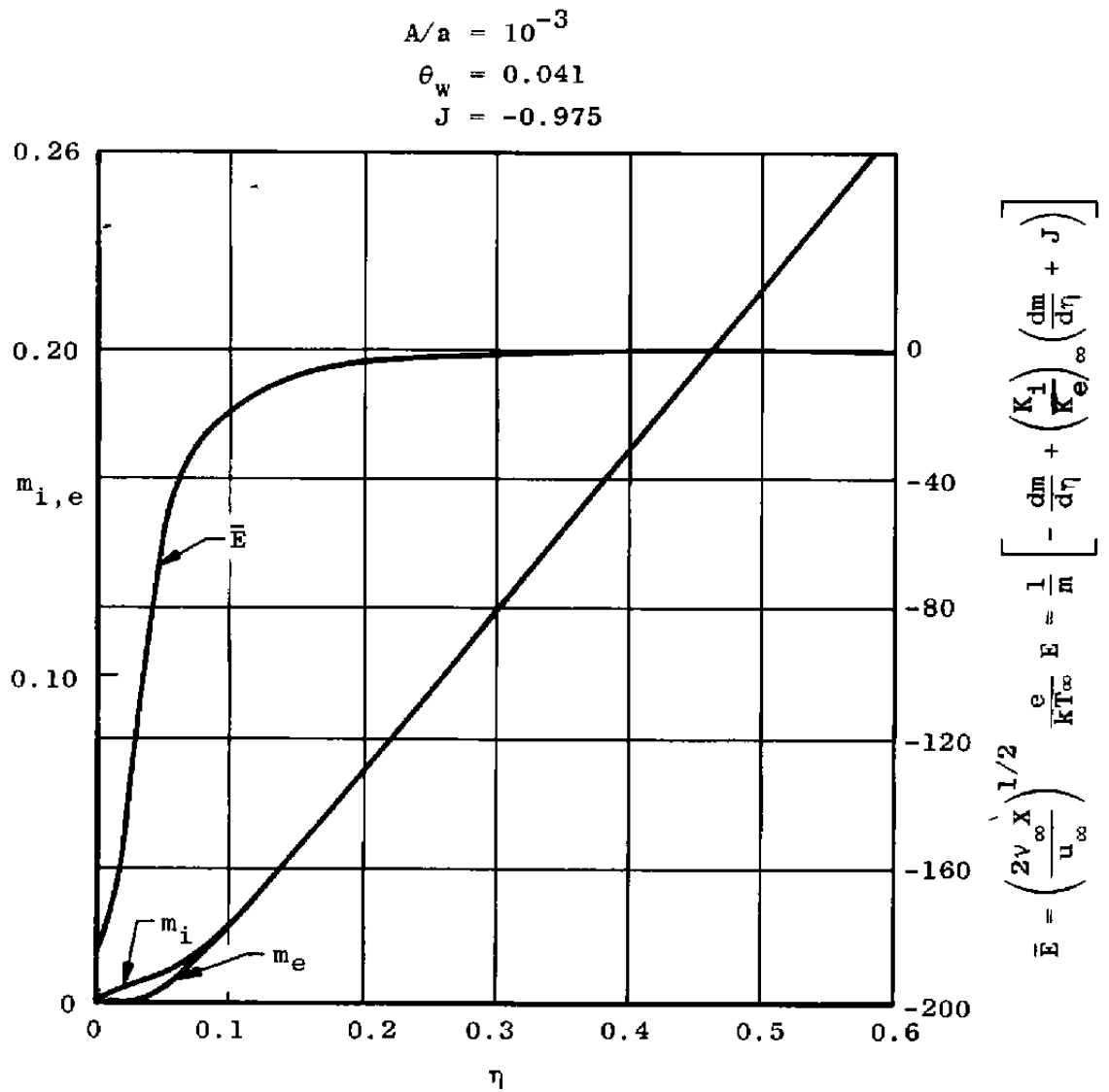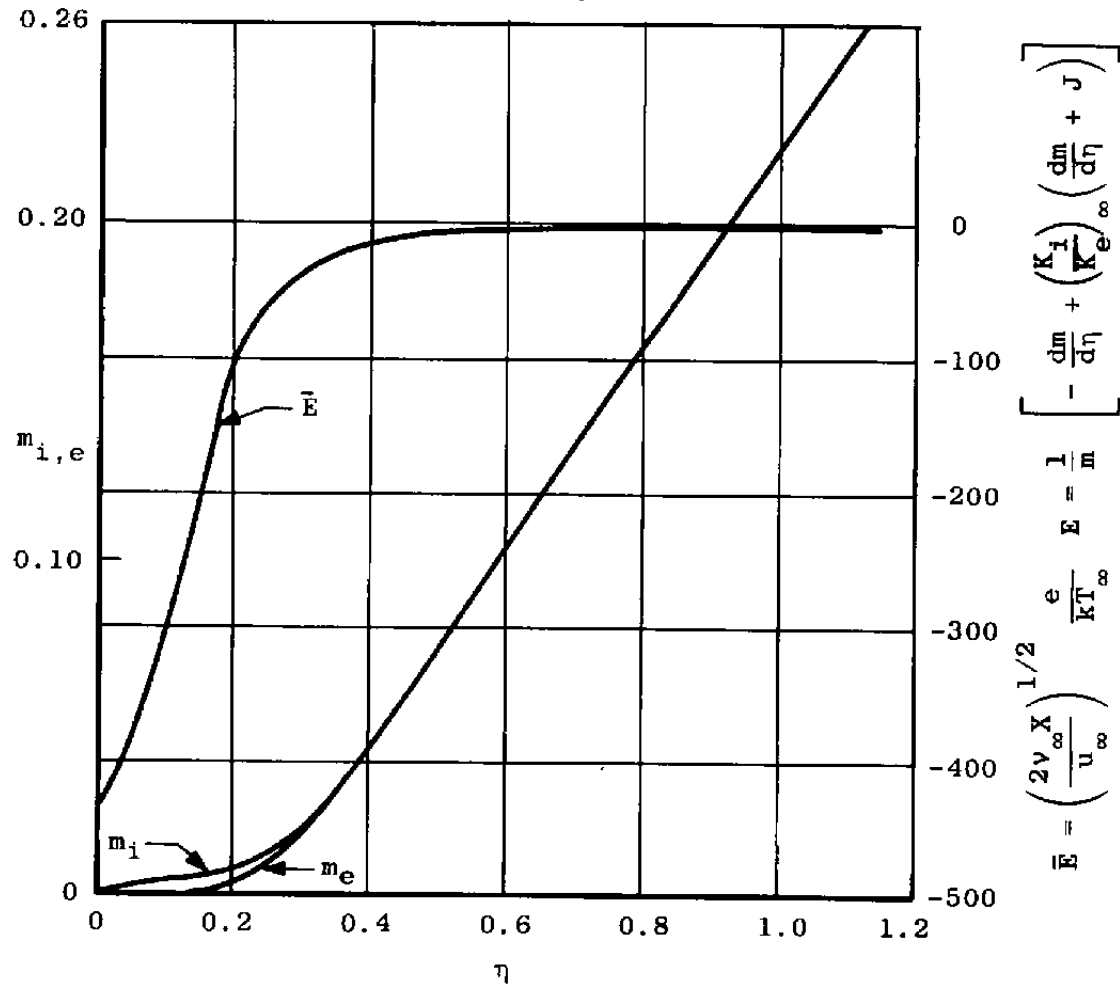a. Equilibrium Boundary Layer

Fig. 7 Number Density and Electric Field Boundary-Layer Profiles

b. Constant Electron Temperature Boundary Layer

Fig. 7 Concluded

J

-0.8

-0.6

-0.4

-0.2

0

0.2

0.4

0.6

$\theta_w = 0.10$
$S_w = 1.00$

$M'_\infty < 1$
$\omega_\infty = 1.00$
$\alpha = 2 \times 10^8$
$\theta_w = 0.10$
$S_w = 1.00$

Sheath

Sheath Plus
Boundary Layer
Equilibrium

Nonequilibrium

Sheath

Sheath plus
Boundary Layer

0 -2 -4 -6 -8 -10 -12 -14 -16 -18 -20
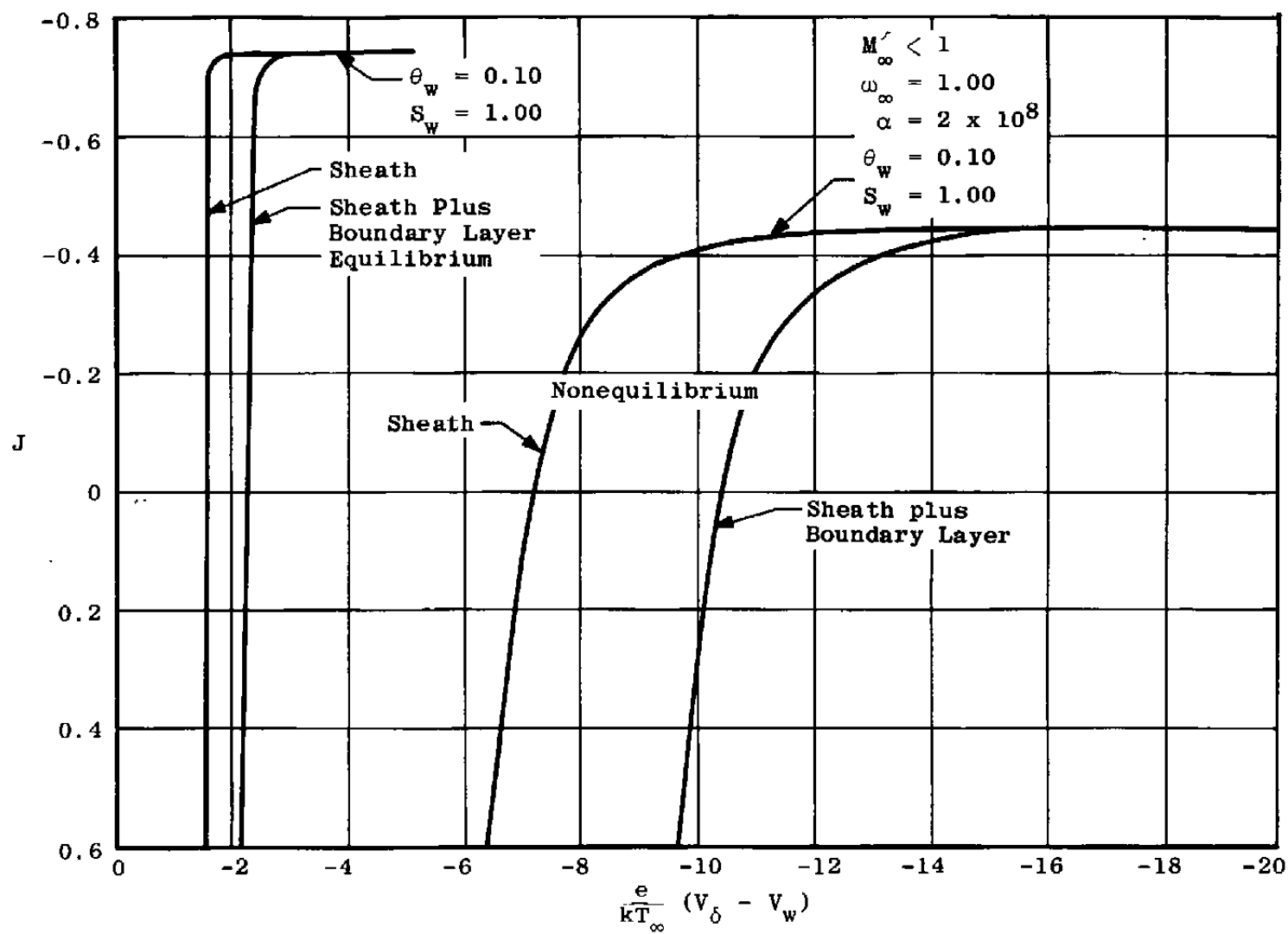
$$\frac{e}{kT_\infty} (V_\delta - V_w)$$

Fig. 8 Voltage Drop for an Equilibrium and Nonequilibrium Sheath and Boundary Layer
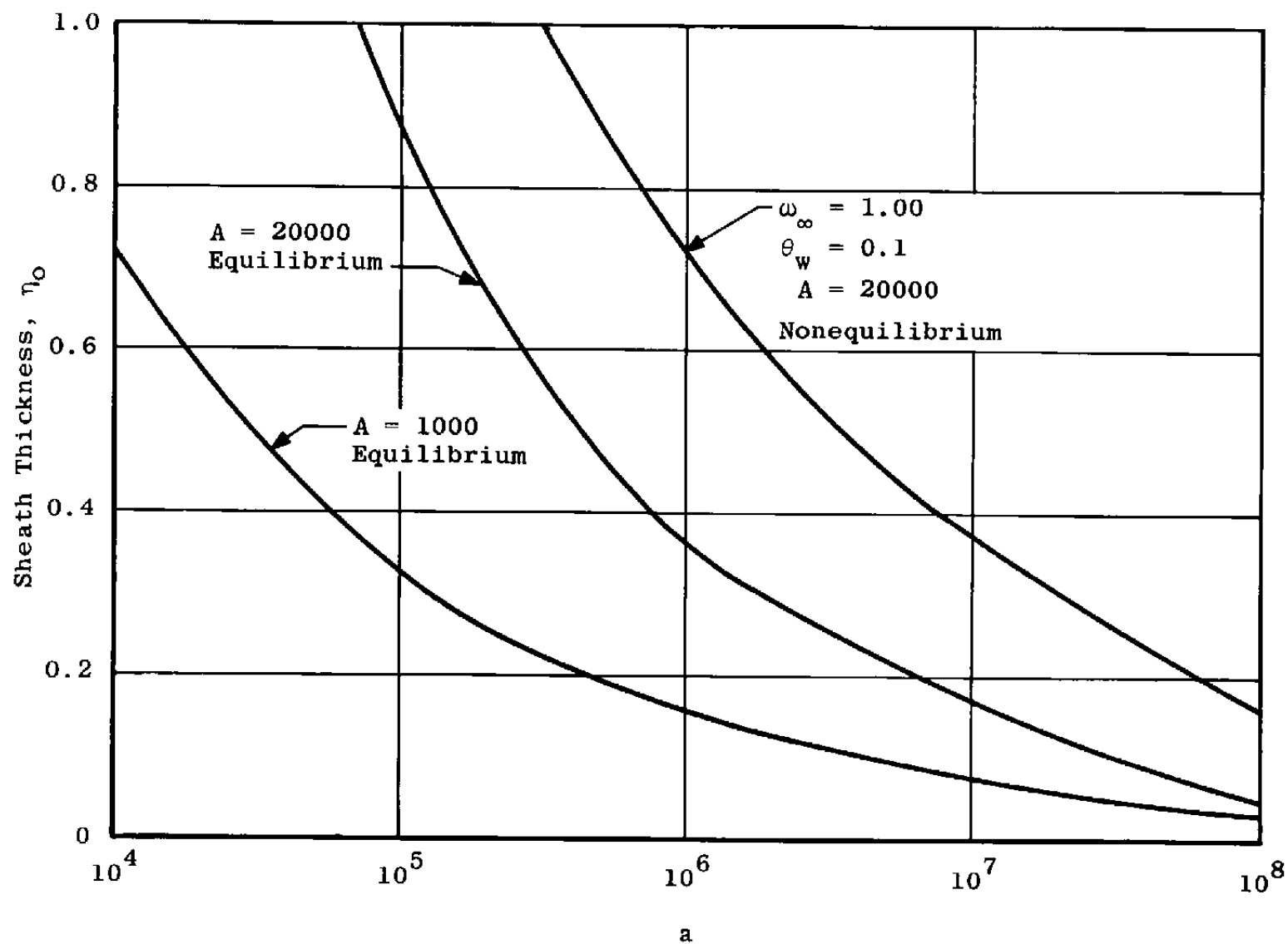
Fig. 9 Sheath Thickness as a Function of the Free-Stream Electron Number Density with Current Saturated
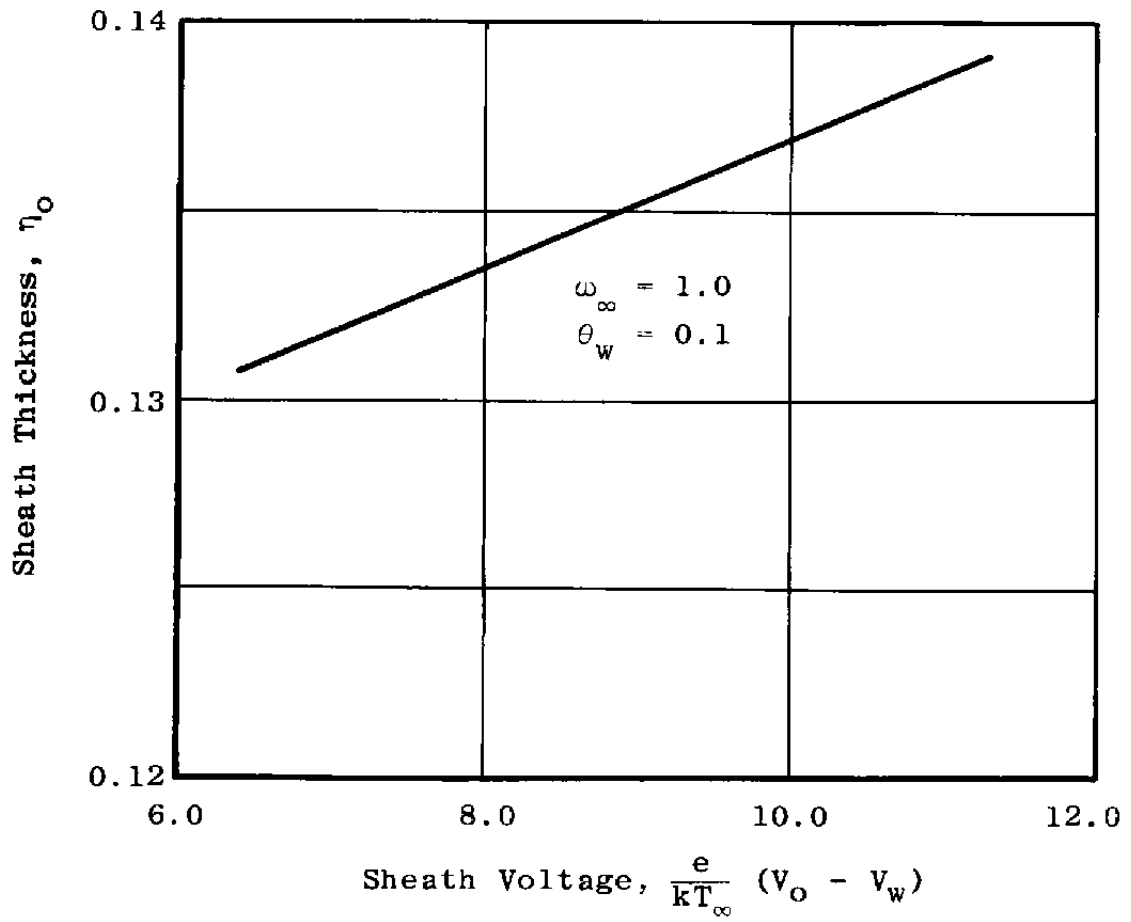
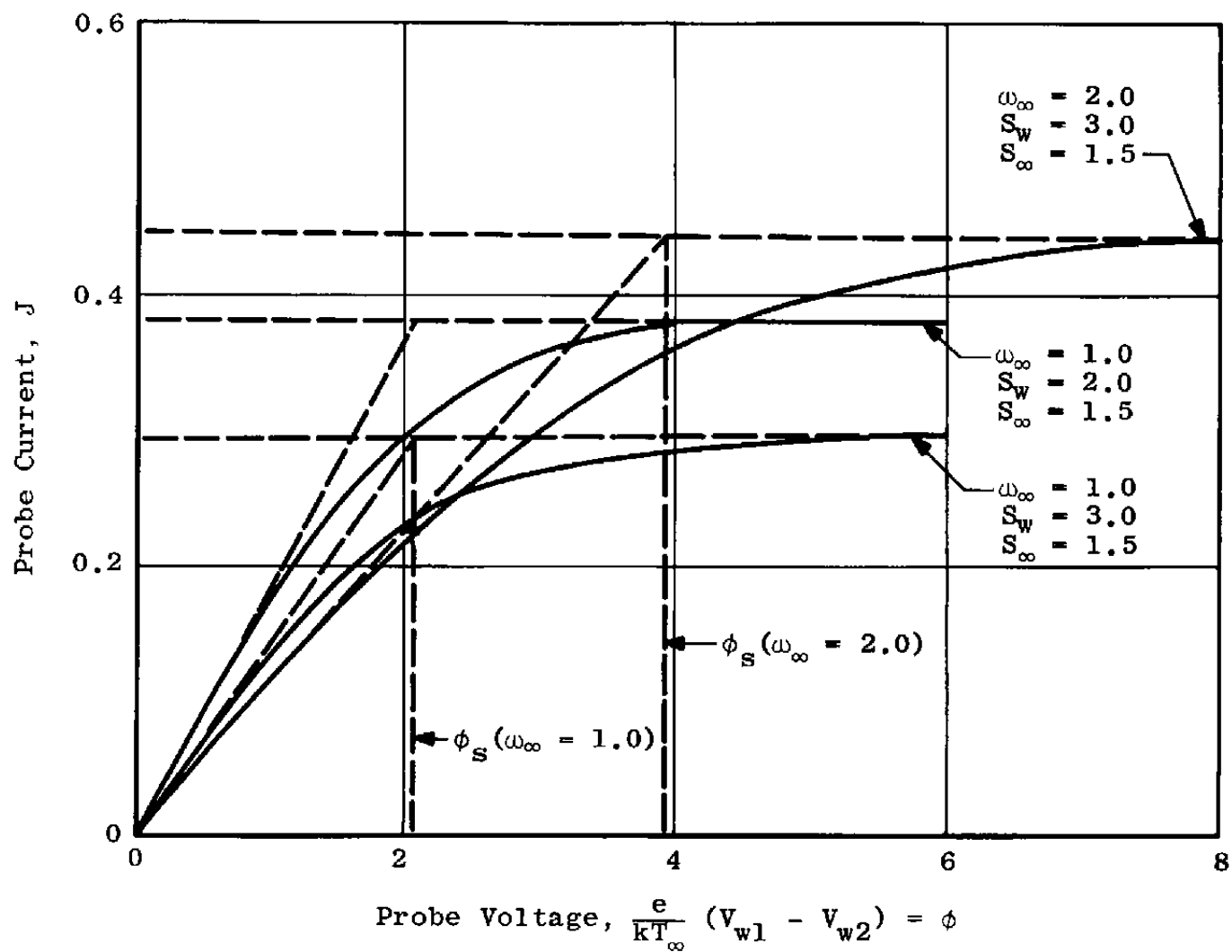Fig. 10 Variation of Sheath Thickness with Sheath Voltage (A/a = 10^{-4})

Fig. 11 Current-Voltage Characteristics for a Double Parallel-Plate Probe
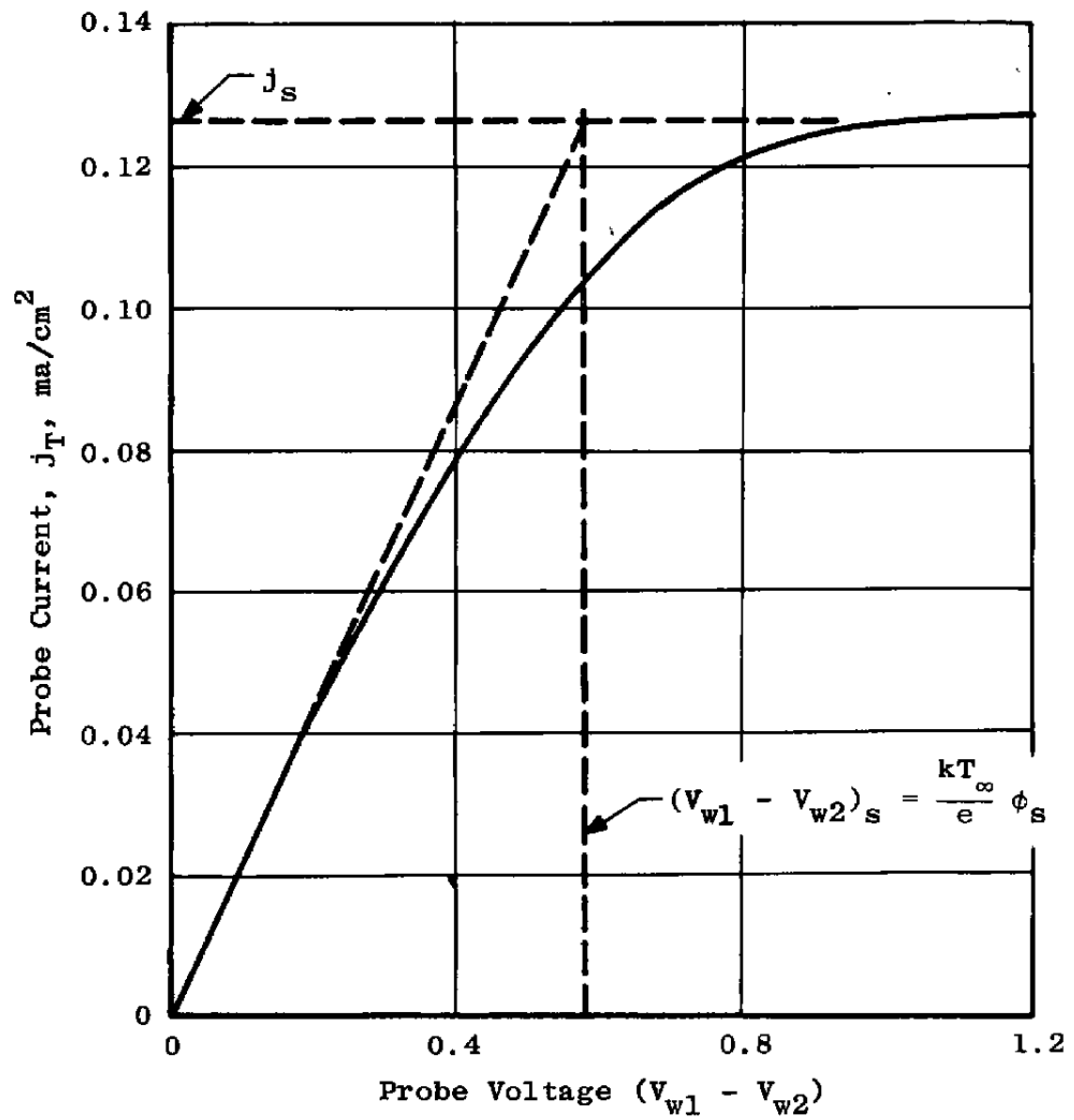
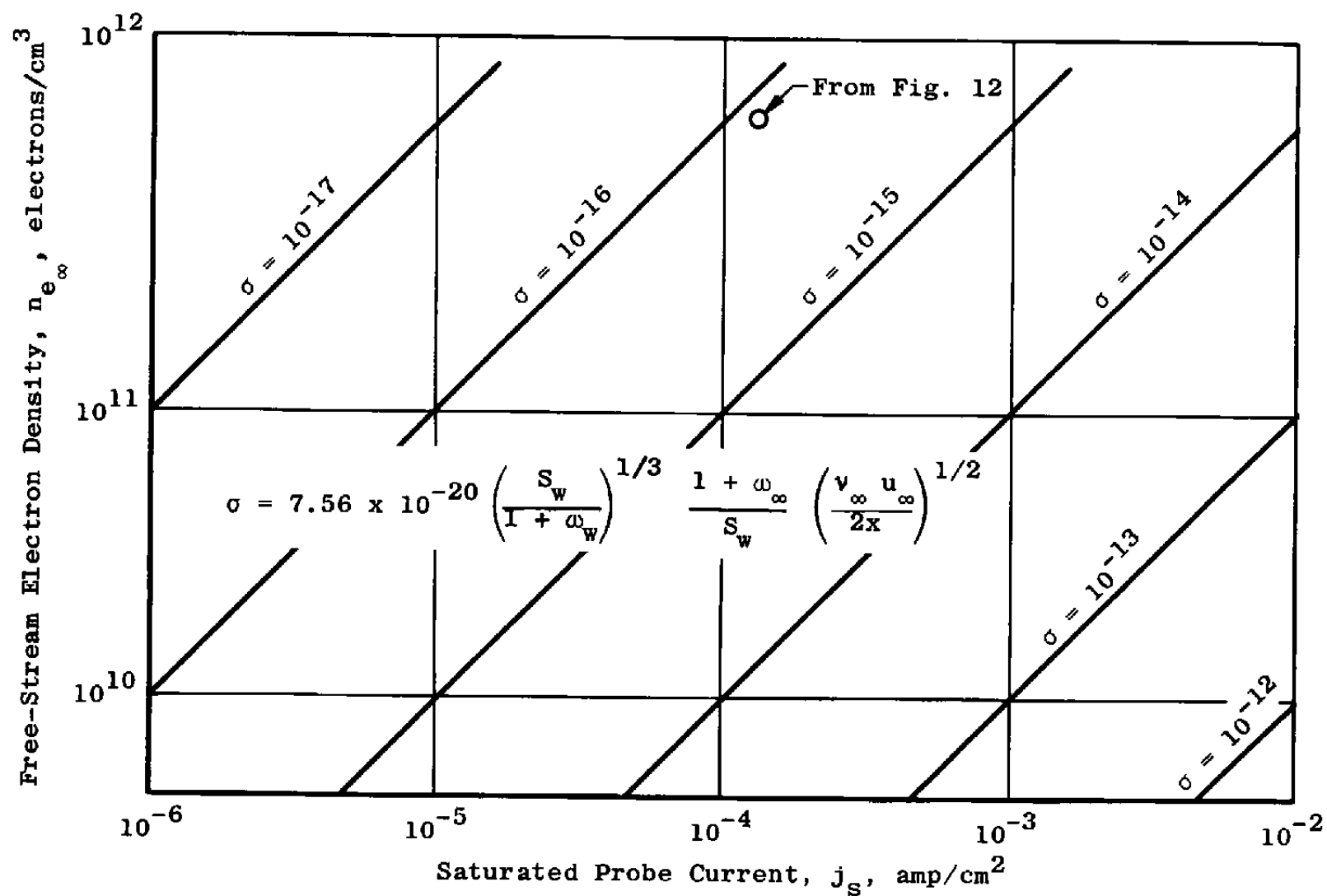Fig. 12 Typical Probe Current-Voltage Characteristic

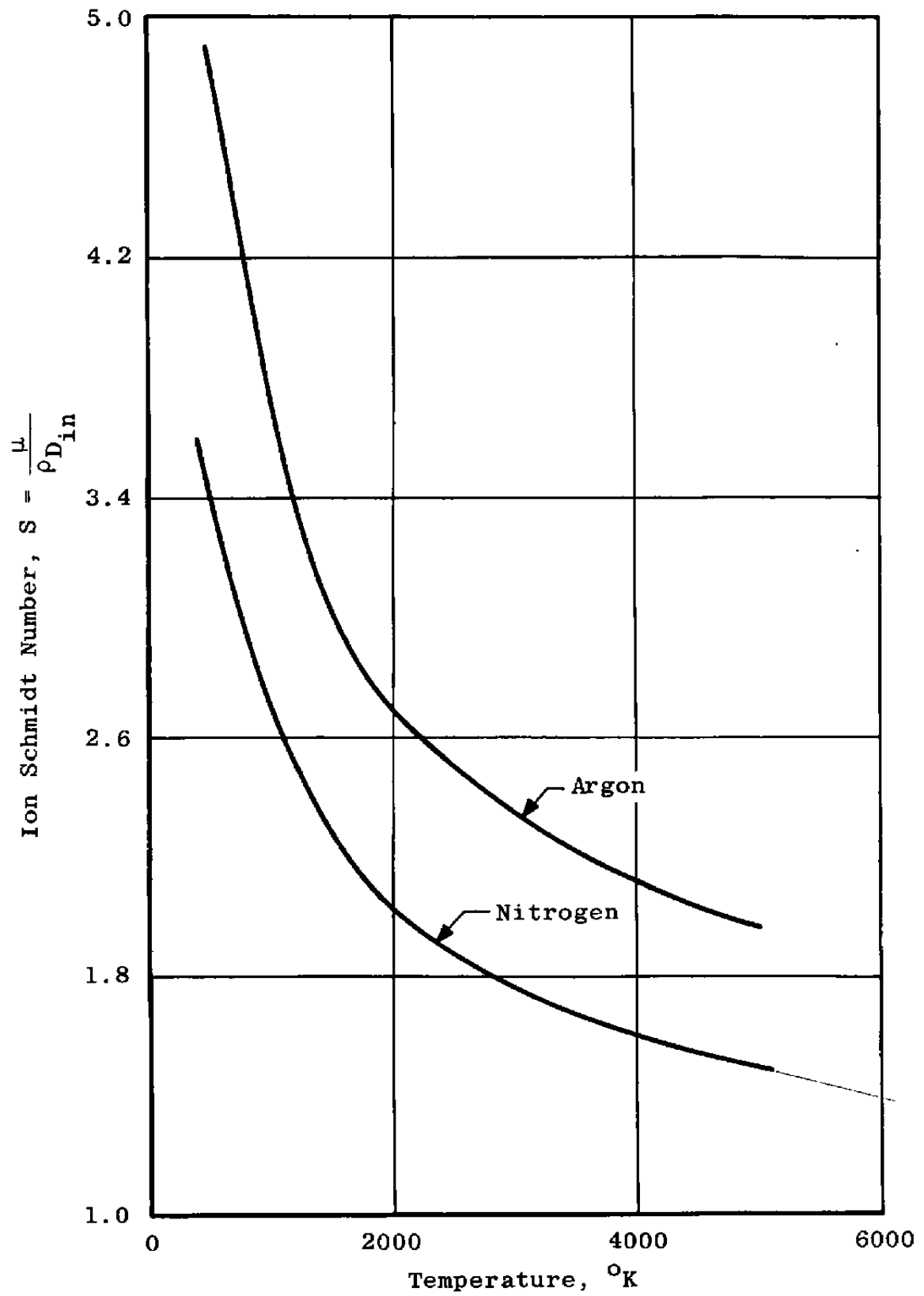Fig. 13 Variation of Ion Saturation Current with Free-Stream Electron Density

Fig. 14 Variation of Ion Schmidt Number with Temperature

APPENDIX II
SIMPLIFIED SHEATH EQUATIONS

EQUILIBRIUM ELECTRON TEMPERATURE

In Section III it was pointed out that the integrals in Eqs. (27) and (28) could be evaluated in terms of the generalized Kummer functions. However, in the cases of interest in this paper these integrals may be simplified and evaluated in terms of much simpler functions. Equations (27) and (28) are:

$$\alpha_i(t) = - J_1 t^{\frac{\gamma_2 A}{3}} e^t \left(\frac{2\gamma_3}{3A^2} \right)^{1/3}$$

$$\int_{t_w}^{t} \left[\frac{\gamma_2 A}{3t} + 1 \right] t^{-\frac{(A\gamma_2 + 1)}{3}} e^{-t} dt \qquad (II-1)$$

$$\alpha_e(t) = - J_1 \bar{k} t^{-\frac{\gamma_2 A}{3}} e^{-t} \left(\frac{2\gamma_3}{3A^2} \right)^{1/3}$$

$$\int_{t_w}^{t} \left[\frac{\gamma_2 A}{3t} + 1 \right] t^{\frac{A\gamma_2 - 1}{3}} e^t dt \qquad (II-2)$$

where

$$\gamma_2 = \frac{1}{A} \left(\frac{1 - \bar{k}}{1 + \bar{k}} \right)$$

$$\gamma_3 = \frac{A}{2J_1 (1 + \bar{k})}$$

Since $\bar{k}$ is 10^{-2} or less for most conditions,

$$-\frac{A\gamma_2 + 1}{3} = -\frac{2}{3(1 + \bar{k})} \approx -\frac{2}{3} \qquad \text{(II-3)}$$

$$\frac{\gamma_2 A}{3} = \frac{1}{3}\left(\frac{1 - \bar{k}}{1 + \bar{k}}\right) \approx \frac{1}{3} \qquad \text{(II-4)}$$

$$-\frac{1}{3}(4 + A\gamma_2) = -\frac{5 + 3\bar{k}}{3(1 + \bar{k})} \simeq -\frac{5}{3} \qquad \text{(II-5)}$$

Using the above approximations in Eq. (II-1) gives

$$\alpha_i(t) \simeq \frac{J_1}{2A}\left(-\frac{1}{R}\right)\left\{\left[\left(\frac{t}{t_w}\right)^{2/3} e^{t - t_w} - 1\right]\right.$$

$$\left. + e^t\ t^{2/3}\left[\gamma\left(\frac{1}{3}, t\right) - \gamma\left(\frac{1}{3}, t_w\right)\right]\right\} \qquad \text{(II-6)}$$

In Eq. (II-2) we let

$$\frac{A\gamma_2 - 4}{3} = -\frac{3 + 5\bar{k}}{3(1 + \bar{k})} \approx -1 \qquad \text{(II-7)}$$

$$\frac{A\gamma_2 - 1}{3} = \frac{-2\bar{k}}{3(1 + \bar{k})} \approx 0 \qquad \text{(II-8)}$$

which gives

$$\alpha_e(t) \simeq \frac{J_1\bar{k}}{A}\left(\frac{1}{R}\right)\left[\frac{e^{-t}}{3}\left(E_i(t) - E_i(t_w)\right)\right.$$

$$\left. + \left(1 - e^{t_w}\right)\right] \qquad \text{(II-9)}$$

where $E_i(t)$ is the exponential integral. Making Eqs. (II-6) and (II-9) satisfy the boundary conditions

$$\alpha_i = 1.0; \quad \alpha_e = 1.0; \quad \zeta = 1.0$$

and using the approximation in Eq. (24) evaluated at $\zeta = 0$ gives three equations for the unknowns J_1, R_w, and R_o.

If the asymptotic expression for large A given in Eq. (23) is used for R_o, Eqs. (II-6), (II-9), and (24), respectively, reduce to

$$R_o \simeq -\frac{J_1(1 - \bar{k})}{2A} \qquad (II-10)$$

$$e^{t_w} \simeq \frac{1 - \bar{k}}{2\bar{k}} \qquad (II-11)$$

and

$$J_1 \simeq 2 + \frac{(3J_1)^{2/3} t_w^{1/3}}{2A^{1/3}(1 + \bar{k})^{1/3}} \left[1 - \frac{2}{3}\frac{1 - \bar{k}}{1 + \bar{k}}\frac{1}{t_w} \right] \qquad (II-12)$$

The equilibrium sheath solution for J_1, R_w, and R_o comes from solving Eqs. (II-10), (II-11) and (II-12). In order to obtain the profiles in Fig. 4, Eqs. (II-6) and (II-9) must be used.

It should be pointed out that the R_w found is an approximation, and the exact value of R at $\zeta = 0$ can be found from Eq. (20),

$$R_w^2 = \frac{4}{A}\left(\frac{J_1(1 + \bar{k})}{2} - 1 \right) + R_o^2 \qquad (II-13)$$

CONSTANT ELECTRON TEMPERATURE

The constant electron temperature case is treated similar to the equilibrium case. Equations (33) and (34) are:

$$\alpha_i(t) = -J_1 t^{\frac{A\gamma_2}{3}} e^t \left(\frac{2\gamma_3}{3A^2} \right)^{1/3}$$

$$\int_{t_w}^{t} \left[\frac{\gamma_2 A}{3t} + 1 \right] t^{-\frac{(A\gamma_2 + 1)}{3}} e^{-t} dt \qquad (II-14)$$

$$\omega\alpha_e(t) = -J_1 \bar{k} \, t^{-\frac{A\beta_2}{\gamma_3}} \, e^{-\frac{\beta_3 t}{\gamma_3}} \left(\frac{2\gamma_3}{3A^2}\right)^{1/3}$$

$$\int_{t_w}^{t} \left[\frac{\gamma_2 A}{3t} + 1\right] t^{\frac{A\beta_2 - 1}{3}} \, e^{\frac{\beta_3 t}{\gamma_3}} \, dt \tag{II-15}$$

Using the approximation

$$\frac{A\beta_2 - 1}{3} \ll 1$$

and integrating gives

$$\alpha_i(t) = -J_1 \left(\frac{2\gamma_3}{3A^2}\right)^{1/3} \frac{t^{-1/3} A\gamma_2}{A\gamma_2 + 1} \left\{ \left(\frac{t}{t_w}\right)^{\frac{A\gamma_2 + 1}{3}} e^{-t_w} - 1 \right.$$

$$+ \left(\frac{A\gamma_2 - 2}{A\gamma_2}\right) e^t \frac{t^{\frac{A\gamma_2 + 1}{3}}}{3}^{\frac{1}{A\gamma_2}} \tag{II-16}$$

$$\left. \left[\gamma\left(\frac{2}{3} - \frac{A\gamma_2}{3}, t_w\right) - \gamma\left(\frac{2}{3} - \frac{A\gamma_2}{3}, t\right)\right]\right\}$$

$$\omega\alpha_e(t) = -J_1 \bar{k} \, t^{-1/3} \left(\frac{2\gamma_3}{3A^2}\right)^{1/3} \left(\frac{\gamma_3}{\beta_3}\right) \left\{1 - e^{\frac{\beta_3}{\gamma_3}(t_w - t)}\right.$$

$$+ \frac{A\gamma_2 \beta_3}{3\gamma_3} \, e^{-\frac{\beta_3}{\gamma_3} t_w} \left[E_i(\bar{t}) - E_i(\bar{t}_w)\right]\right\} \tag{II-17}$$

where

$$\bar{t} = \frac{\beta_3}{\gamma_3} t$$

The third equation is obtained from Eq. (36) evaluated at $\zeta = 0$:

$$J_1 (1 + \bar{k}) = (1 + \omega_o) + \frac{A}{2} (R_w^2 - R_o^2) \qquad \text{(II-18)}$$

It should be pointed out that γ_2 and γ_3 are not the same as those in the equilibrium solution but are given in Eq. (30). In general, approximations of the type made in the equilibrium electron temperature solution cannot be made in Eqs. (II-16) and (II-17). To obtain the profiles shown in Fig. 5, Eqs. (II-16) and (II-17) have to be used in the form shown. Solving Eqs. (II-16) and (II-17), evaluated at $\zeta = 1.0$, along with Eq. (II-18) completes the constant electron temperature sheath solution.

APPENDIX III
BOUNDARY-LAYER APPROXIMATIONS

A useful method of solving boundary-layer equations is demonstrated in this section. The Blasius equation is

$$f''' + ff'' = 0 \tag{III-1}$$

where the superscript prime denotes differentiation with the variable η. Equation (III-1) can be integrated formally as

$$f' = C_1 \int_0^\eta e^{-\int_0^\eta f d\eta} d\eta + C_2 \tag{III-2}$$

Applying the boundary conditions of $f'(o) = 0$ and $f' = 1.0$ as $\eta \to \infty$ gives

$$f' = \frac{\displaystyle\int_0^\eta e^{-\int_0^\eta f d\eta} d\eta}{\displaystyle\int_0^\infty e^{-\int_0^\eta f d\eta} d\eta} \tag{III-3}$$

Here f' can be evaluated for any assumed f. Since the exponential rapidly decays as η becomes larger, the integration weights f heavily near the wall ($\eta = 0$). For cases of no slip and no suction and/or blowing at the wall, the velocity profile is almost linear near the wall. This implies

$$f' = f''_w \eta$$

which in turn gives

$$f = \frac{f''_w}{2} \eta^2$$

Substituting this relation into Eq. (III-3) and integrating gives

$$f' = \frac{\gamma\left(\dfrac{1}{3}; \dfrac{f''_w}{6} \eta^3\right)}{\Gamma\left(\dfrac{1}{3}\right)} \tag{III-4}$$

where $\gamma\left(\dfrac{1}{3},x\right)$ is the incomplete gamma function.

In order to check the accuracy of the approximation, differentiate Eq. (III-4) and evaluate the derivative at $\eta = 0$

$$f''(o) = f''_w = \frac{3}{\Gamma\left(\dfrac{1}{3}\right)}\left(\frac{f''_w}{6}\right)^{1/3}$$

This gives $f''_w = 0.480$ which compares to $f''_w = 0.470$ for numerical solutions. Hence, Eq. (III-4) is seen to be a good approximation for the velocity profile.

Since f''_w is known for numerical solutions, a better approximation to f' may be found by making it satisfy the condition $f''(o) = f''_w = 0.470$. Using this condition rather than $f' = 1.0$ as $\eta \to \infty$ gives

$$f' = \frac{f''_w}{3}\left(\frac{6}{f''_w}\right)^{1/3}\ \gamma\left(\frac{1}{3},\ \frac{f''_w}{6}\ \eta^3\right) \qquad \text{(III-5)}$$

which agrees well with numerical solutions of f' for all η, differing by only two percent as $\eta \to \infty$. Equation (III-5) implies that

$$f'' = f''_w\ \exp\left(-\ \frac{f''_w}{6}\ \eta^3\right)$$

is a good approximation to f'' for all η and can be used in obtaining solutions for other quantities in boundary-layer convection-diffusion equations.

APPENDIX IV
RANGE OF VALIDITY OF THE THEORY

An examination will be made here of the assumptions given in Section II to show the approximate range of validity for the theory presented in this report. The three most critical assumptions are examined in more detail below.

FROZEN FLOW

The flow is assumed to be frozen in ionization and recombination both while the particles diffuse through the boundary layer and are convected along the plate. The characteristic times for these two phenomena are approximately the same; therefore we need consider only the convection along the plate.

The resident time for a particle in the free stream is

$$\tau = \frac{L}{u_\infty} \text{ sec} \tag{IV-1}$$

The characteristic reaction for air is the dissociative-recombination of NO^+. The rate coefficient for this is given in Ref. 8 with a resulting time for recombination of

$$\tau_{rec} = \frac{10 \ T_e^{3.5}}{n_{e_\infty}} \text{ sec} \tag{IV-2}$$

For argon, three-body recombination normally dominates; the rate coefficient from Ref. 19 gives,

$$\tau_{rec} = 3.01 \cdot 10^{12} \ \frac{T_e^{2.94}}{n_{e_\infty}^2} \text{ sec} \tag{IV-3}$$

For the assumption of frozen flow to be valid we require

$$\frac{\tau}{\tau_{rec}} < 1$$

which gives an electron number density limit for air

$$n_{e_\infty} < \frac{u_\infty}{L} \ 10^6 \ \frac{T_e^{3.5}}{10^5} \tag{IV-4}$$

and for argon,

$$n_{e_\infty} < 1.76 \times 10^{12} \sqrt{\frac{u_\infty}{L}} \; T_e^{1.47} \qquad \text{(IV-5)}$$

In these equations T is in °K, L is in m, u_∞ is in m/sec, and n_{e_∞} is in particles/m^3.

NEGLIGIBLE CONVECTION IN SHEATH

It is assumed that the convective contribution to the current normal to the wall is negligible in the sheath. If the convective terms are retained in the sheath, Eqs. (14) and (15) become (for $T_e = T$):

$$\frac{d\alpha_i}{d\zeta} - A\alpha_i R = J_1 - S_w \, \eta_o \int_o^\zeta f \, \frac{d\alpha_i}{d\zeta} \, d\zeta \qquad \text{(IV-6)}$$

$$\frac{d\alpha_e}{d\zeta} + A\alpha_e R = J_1 \bar{k} - S_w \left(\frac{K_i}{K_e}\right)_\infty \eta_o \int_o^\zeta f \, \frac{d\alpha_e}{d\zeta} \, d\zeta \qquad \text{(IV-7)}$$

Since the maximum contribution of convection occurs at the edge of the sheath ($\zeta = 1$), the convective terms are approximated using

$$f \simeq \frac{f_w''}{2} \eta^2 = \frac{f_w''}{2} \eta_o^2 \zeta^2$$

and (see for example Fig. 4)

$$\alpha_{i,e} \simeq \zeta$$

The integration then gives

$$\frac{d\alpha_i}{d\zeta} - A\alpha_i R = J_1 \left[1 - S_w \frac{f_w''}{6} \frac{\eta_o^3}{J_1} \zeta^3 \right] \qquad \text{(IV-8)}$$

and

$$\frac{d\alpha_e}{d\zeta} + A\alpha_e R = J_1 \bar{k} \left[1 - S_w \left(\frac{K_1}{K_e}\right)_\infty \frac{f_w''}{6} \frac{\eta_o^3}{J_1 \bar{k}} \zeta^3 \right] \qquad (IV-9)$$

The terms on the left-hand side of Eqs. (IV-8) and (IV-9) are approximately equal to unity. A comparison of the convective term from Eq. (IV-8) with unity gives,

$$\eta_o < \left(\frac{6}{f_w'' S_w}\right)^{1/3} \qquad (IV-10)$$

and from Eq. (IV-9)

$$\eta_o < \left(\frac{K_1}{K_e}\right)_\infty^{1/3} \left(\frac{6}{f_w'' S_w}\right)^{1/3}$$

Since $\qquad \left(\frac{K_1}{K_e}\right)_\infty^{1/3} \simeq \left(\frac{M_1}{M_e}\right)^{1/6} \simeq 6$

it is seen that convection is never important in determining the flow of the electrons to the wall. The ion current dominates as saturation is reached (and the sheath thickens); hence we shall use Eq. (IV-10) as the criterion to determine at what point in the boundary-layer convection may be neglected.

SHEATH THICKNESS LARGER THAN AN ELECTRON-NEUTRAL MEAN FREE PATH

The assumption that the sheath thickness is larger than an electron-neutral mean free path requires that:

$$\eta_o > \left(\frac{u_\infty}{2\nu_\infty x}\right)^{1/2} \int_o^\lambda \frac{\rho}{\rho_\infty} \, dy \simeq \left(\frac{u_\infty}{2\nu_\infty x}\right)^{1/2} \frac{\rho_w}{\rho_\infty} \lambda$$

Taking the mean free path to be

$$\lambda = \frac{1}{n_w Q_{en}}$$

we see that

$$\eta_o > \left(\frac{u_\infty}{2\nu_\infty x} \right)^{1/2} \frac{1}{\rho_\infty} \frac{M}{Q_{en}} , \qquad \text{(IV-12)}$$

where M is the mass of the neutral particle and Q_{en} is the effective collision cross section for momentum transfer.

It is found that all the charge separation is contained well within the sheath when $A \geq 1000$. This fact is also pointed out by Chung in Ref. 5. From the definition of A we have

$$n_{e_o} = \frac{\varepsilon_o k T_o}{e^2} \frac{A}{\eta_o^2} \left(\frac{\rho_o}{\rho_\infty} \right)^2 \left(\frac{u_\infty}{2\nu_\infty x} \right)$$

Using Eq. (52) we let

$$\frac{\rho_\infty n_{e_o}}{\rho_o n_{e_\infty}} = m_o \sim \left(\frac{S_w}{2} \right)^{1/3} f_w'' \eta_o$$

to eliminate n_{e_o} from the above equation; hence

$$n_{e_\infty} \simeq \frac{\varepsilon_o k T_\infty}{e^2} \left(\frac{2}{S_w} \right)^{1/3} \frac{A}{f_w'' \eta_o^3} \left(\frac{u_\infty}{2\nu_\infty x} \right) \qquad \text{(IV-13)}$$

We may now put the criteria developed in the preceding two sections into Eq. (IV-13) to give the limits on n_{e_∞}.

For convection to be negligible we find by substituting Eq. (IV-10) into Eq. (IV-13)

$$n_{e_\infty} > 1.57 \cdot 10^6 \left(\frac{S_w}{2} \right)^{2/3} \left(\frac{u_\infty}{2\nu_\infty x} \right) T_\infty \qquad \text{(IV-14)} \checkmark$$

For the sheath to be larger than the electron-neutral mean free path we find by substituting Eq. (IV-12) in Eq. (IV-13)

$$n_{e_\infty} < 1.16 \cdot 10^{30} \frac{\rho_\infty^3}{T_\infty^2} \left(\frac{2\nu_\infty x}{u_\infty} \right)^{1/2} \left[\text{argon} \right] \qquad \text{(IV-15a)}$$

$$n_{e_\infty} < 3.80 \cdot 10^{33} \frac{p_\infty^3}{T_\infty^2} \left(\frac{2\nu_\infty x}{u_\infty} \right)^{1/2} \left[air \right] \qquad \text{(IV-15b)}$$

where p_∞ is an atm and other quantities are in MKS units.

The applicability of the continuum electrostatic flat plate probe to a given flow can be determined from Eqs. (IV-4), (IV-5), (IV-14) and (IV-15) taken collectively.

DOCUMENT CONTROL DATA - R&D

(Security classification of title, body of abstract and indexing annotation must be entered when the overall report is classified)

1 ORIGINATING ACTIVITY *(Corporate author)*	2a REPORT SECURITY CLASSIFICATION
Arnold Engineering Development Center ARO, Inc., Operating Contractor Arnold Air Force Station, Tennessee	UNCLASSIFIED
	2b GROUP N/A

3 REPORT TITLE

ANALYTICAL SOLUTIONS FOR A CONTINUUM PARALLEL-PLATE ELECTROSTATIC PROBE

4 DESCRIPTIVE NOTES *(Type of report and inclusive dates)*

N/A

5 AUTHOR(S) *(Last name, first name, initial)*

High, Michael D., ARO, Inc.

6 REPORT DATE	7a TOTAL NO OF PAGES	7b. NO OF REFS
May 1967	73	19

8a CONTRACT OR GRANT NO AF 40(600)-1200	9a ORIGINATOR'S REPORT NUMBER(S)
b PROJECT NO. 5730	AEDC-TR-67-71
c Program Element 62405184	9b OTHER REPORT NO(S) *(Any other numbers that may be assigned this report)*
d	N/A

10 AVAILABILITY/LIMITATION NOTICES Distribution of this document is unlimited. It may be released to the Clearinghouse, Department of Commerce, for sale to the general public.

11 SUPPLEMENTARY NOTES Available in DDC.	12 SPONSORING MILITARY ACTIVITY Arnold Engineering Development Center Air Force Systems Command Arnold Air Force Station, Tennessee

13 ABSTRACT

    The theory for the flow of a weakly ionized gas through a parallel-plate, continuum, electrostatic probe is developed. The flow is separated into three distinct regions: (a) the inviscid, neutral core where electron conduction maintains the continuity of current between the two plates; (b) the viscous, quasi-neutral boundary layer in which the charged particle flow is similar to ambipolar diffusion; and (c) the one-dimensional, collision dominated, space-charge sheath. Analytical solutions, matched at the boundary of each region, are presented for the electron temperature in equilibrium with the gas temperature and for the electron temperature constant at its free-stream value. A criterion is given which may be used to determine whether electron thermal equilibrium exists through the boundary layer. It is shown that the sheath voltage drop comprises approximately 60 percent of the total plate voltage drop. The results also show a very well defined saturation current for the double probe and that this current is controlled by ion diffusion through the boundary layer. Expressions are developed from the solutions which allow the use of experimental data to determine the free-stream electron density and temperature.

DD FORM 1 JAN 64 1473

14 KEY WORDS	LINK A		LINK B		LINK C	
	ROLE	WT	ROLE	WT	ROLE	WT
electrostatic probes mathematical analysis gas flow analysis						

INSTRUCTIONS

1. **ORIGINATING ACTIVITY:** Enter the name and address of the contractor, subcontractor, grantee, Department of Defense activity or other organization (*corporate author*) issuing the report.

2a. **REPORT SECURITY CLASSIFICATION:** Enter the overall security classification of the report. Indicate whether "Restricted Data" is included. Marking is to be in accordance with appropriate security regulations.

2b. **GROUP:** Automatic downgrading is specified in DoD Directive 5200.10 and Armed Forces Industrial Manual. Enter the group number. Also, when applicable, show that optional markings have been used for Group 3 and Group 4 as authorized.

3. **REPORT TITLE:** Enter the complete report title in all capital letters. Titles in all cases should be unclassified. If a meaningful title cannot be selected without classification, show title classification in all capitals in parenthesis immediately following the title.

4. **DESCRIPTIVE NOTES:** If appropriate, enter the type of report, e.g., interim, progress, summary, annual, or final. Give the inclusive dates when a specific reporting period is covered.

5. **AUTHOR(S):** Enter the name(s) of author(s) as shown on or in the report. Enter last name, first name, middle initial. If military, show rank and branch of service. The name of the principal author is an absolute minimum requirement.

6. **REPORT DATE:** Enter the date of the report as day, month, year; or month, year. If more than one date appears on the report, use date of publication.

7a. **TOTAL NUMBER OF PAGES:** The total page count should follow normal pagination procedures, i.e., enter the number of pages containing information.

7b. **NUMBER OF REFERENCES:** Enter the total number of references cited in the report.

8a. **CONTRACT OR GRANT NUMBER:** If appropriate, enter the applicable number of the contract or grant under which the report was written.

8b, 8c, & 8d. **PROJECT NUMBER:** Enter the appropriate military department identification, such as project number, subproject number, system numbers, task number, etc.

9a. **ORIGINATOR'S REPORT NUMBER(S):** Enter the official report number by which the document will be identified and controlled by the originating activity. This number must be unique to this report.

9b. **OTHER REPORT NUMBER(S):** If the report has been assigned any other report numbers (*either by the originator or by the sponsor*), also enter this number(s).

10. **AVAILABILITY/LIMITATION NOTICES:** Enter any limitations on further dissemination of the report, other than those imposed by security classification, using standard statements such as:

(1) "Qualified requesters may obtain copies of this report from DDC."

(2) "Foreign announcement and dissemination of this report by DDC is not authorized."

(3) "U. S. Government agencies may obtain copies of this report directly from DDC. Other qualified DDC users shall request through

_____ ."

(4) "U. S. military agencies may obtain copies of this report directly from DDC. Other qualified users shall request through

_____ ."

(5) "All distribution of this report is controlled. Qualified DDC users shall request through

_____ ."

If the report has been furnished to the Office of Technical Services, Department of Commerce, for sale to the public, indicate this fact and enter the price, if known.

11. **SUPPLEMENTARY NOTES:** Use for additional explanatory notes.

12. **SPONSORING MILITARY ACTIVITY:** Enter the name of the departmental project office or laboratory sponsoring (*paying for*) the research and development. Include address.

13. **ABSTRACT:** Enter an abstract giving a brief and factual summary of the document indicative of the report, even though it may also appear elsewhere in the body of the technical report. If additional space is required, a continuation sheet shall be attached.

It is highly desirable that the abstract of classified reports be unclassified. Each paragraph of the abstract shall end with an indication of the military security classification of the information in the paragraph, represented as (TS), (S), (C), or (U)

There is no limitation on the length of the abstract. However, the suggested length is from 150 to 225 words.

14. **KEY WORDS:** Key words are technically meaningful terms or short phrases that characterize a report and may be used as index entries for cataloging the report. Key words must be selected so that no security classification is required. Identifiers, such as equipment model designation, trade name, military project code name, geographic location, may be used as key words but will be followed by an indication of technical context. The assignment of links, rules, and weights is optional.